DETERMINATION OF LONGITUDINAL DISPERSION COEFFICIENT OF A CHANNEL HAVING RIGID VEGETATION

A Dissertation Submitted
In Partial Fulfillment of the Requirements
for the degree of

MASTERS OF ENGINEERING
IN
CIVIL INFRASTRUCTURE ENGINEERING

Submitted by:
VISHAL KUMAR DHIMAN
(ROLL NO. 801523014)

UNDER THE SUPERVISION OF

DR. DWARIKANATH RATHA
Associate Professor
Department. of Civil Engineering
Thapar University, Patiala

DR. RICHA BABBAR
Assistant Professor
Department. of Civil Engineering
Thapar University, Patiala

DEPARTMENT OF CIVIL ENGINEERING
THAPAR UNIVERSITY,
PATIALA-147004

JULY 2017

DECLARATION

I, Vishal Kumar Dhiman, hereby declare that this thesis entitled **"Determination of Longitudinal Dispersion Coefficients of a channel having Rigid Vegetation"** is an authentic record of my study carried out asrequirements for the award of degree of **Master of Engineering** in **Infrastructure Engineering** in the Civil Engineering Department, Thapar University, Patiala under the supervision of **Dr. Dwarikanath Ratha**, **Associate Professor and Dr. Richa Babbar, Assistant Professor,** Department of Civil Engineering, Thapar University, Patiala during July 2015 to July 2017. This matter embodied in this report has not been submitted in part or full to any other university or institute for the award of any degree.

Date: 20/07/2017

(Vishal Kumar Dhiman)
Roll No. :801523014

CERTIFICATE

This is to certify that above statement made by the student concerned is correct and true to the best of my knowledge and belief.

20/07/2017

Dr. Dwarikanath Ratha
Associate Professor
Department of Civil Engineering
Thapar University, Patiala

20/7

Dr. Richa Babbar
Assistant Professor
Department of Civil Engineering
Thapar University, Patiala

ACKNOWLEDGMENT

A thesis cannot be completed without the help of many people who contribute directly or indirectly through their constructive criticism in the evolution and preparation of this work. It would not be fair on my part, if I don't say a word of thanks to all those whose sincere advice made this period a real educative, enlightening, pleasurable and memorable one.

I extend my deep sense of gratitude to my supervisions, **Dr. Dwarikanath Ratha, Associate Professor and Dr. Richa Babbar, Assistant Professor,** Department of Civil Engineering, Thapar University, Patiala who permitted me to carry out research work under their able guidance. Their dynamism and diligent enthusiasm has been highly instrumental in keeping my spirit high. Their abundant knowledge in civil and construction field is a benefit for me.

I am extremely thankful to **Mr. Hitesh Singh, Mr. Satya Narayan Singh and Mr. Amarjit Singh**, lab attendant for his kind support in execution of experimental work in the Water Resource Engineering Laboratory of the Department.

I would also like to thank my parents, brother and my classmates for their support and motivation during the entire course of my thesis work.

Vishal Dhiman

Vishal Kumar Dhiman

(801523014)

ABSTRACT

In recent years, aquatic vegetation has become more accepted and important plans for restoration of rivers and preservation of river ecology. The purpose of this thesis is to investigate the effect of vegetation on longitudinal hydrodynamic dispersion and to have a better understanding the effect of vegetation on the mixing processes. To achieve this goal, we performed a series of experiments in an open channel with emergent rigid acrylic tubes of three different diameters in staggered configuration with three different spacing between tubes. The speed measurement of the tracer concentration for nine vegetation densities in 27 numbers of experiments. The coefficient of dispersion is depended on the diameter of rigid vegetation, when a rigid vegetation of different diameter is kept at a distance from point of injection the dispersion coefficient value increases in magnitude and it is inversely related with the density of vegetation till some extent, but it is directly proportional with the diameter of vegetation as the diameter increases the dispersion coefficient is also increases. In vegetation, the longitudinal dispersion is reduced as the vegetation density increases with a reduction of approximately 30% to 50% when the density is doubled. The percentage difference between the mean velocity and the cloud velocity is greater for the lower Reynolds number and this percentage decreases for the higher Reynolds number. The speed at which the cloud propagate that decrease in the maximum concentration and the resulting concentration profile along the stream are of great importance in pollution control. The experiment results obtained in the present study are compared with empirical relationship provided by various researcher. It is found that fischer routing equation has best fit to our present experiment results.

Also, the equation is developed for predicting longitudinal dispersion coefficient having rigid vegetation in channel flow considering the various parameters and found that the coefficient of dispersion depends on the density of the vegetation but depends strongly on the diameter of the vegetation due to the increase of the surface area. The functional relationship between the various parameters obtained using IBM SPSS Statistics and the predicted equation is developed to determine the dispersion coefficient which found to correlate well with the observed dispersion coefficient.

CONTENTS

LIST OF TABLES

LIST OF FIGURES

CHAPTER 1

INTRODUCTION

1.1 Purpose

This study seeks to understand the mechanics of longitudinal dispersal under flow conditions similar to those of natural streams. Longitudinal dispersion is the action by which a stream flow dilutes a mass of pollutants. Rather than moving downstream like a slug, such a mass will be distributed over the entire length of the stream, with some parts moving faster or slower than the average flow velocity. The speed at which the cloud propagates, the decrease in the maximum concentration and the resulting concentration profile along the current are of great importance in controlling pollution. It has been observed that the dispersion characteristics of natural currents vary considerably from one stream to another the individual dispersion characteristics of the flow is also required for the preparation of a rational pollution control program for a particular flow.

1.2 Longitudinal Dispersion

Longitudinal dispersion is the action by which a flow of water flows and dilutes a mass of pollutants. The longitudinal dispersion coefficient is a combined effect of molecular diffusion, turbulent mixing and mixing due to transverse and vertical shear. and have extensively studied longitudinal dispersion.

The longitudinal dispersion coefficient is a key parameter in determining the distribution of pollution concentration particularly in temporally varied source cases after the cross-sectional mixing has taken place. Several studies have been carried out to present simple formulas for this behaviour.

In rivers, longitudinal dispersion becomes the predominant mechanism in the tracer mixture by several orders of magnitude when the cross-sectional mixture is completed. The dispersion coefficient plays an important role in the modelling of spills, the design of water intakes, falls and treatment plants and is representative of the intensity of mixing in rivers. Therefore, an accurate estimate of the coefficient of longitudinal dispersion is of great importance to engineers and scientists. Direct estimation (by experimental means) of the dispersion coefficient requires costly

and time-consuming tracing studies. As a result, the demand for a coefficient prediction tool still exists. The estimation of the longitudinal dispersion coefficient received considerable attention over a long period of time. It is still a difficult task to quantify this coefficient since various governance parameters cause complexity in the mixing process. Therefore, the introduction of mathematical expressions for the dispersion coefficient becomes problematic. Considering that the flows of the river may vary according to their condition, a formula may not produce precise dispersion coefficients. However, this approach is a fairly common practice in the field of hydraulic engineering. When a tracer is introduced into a channel, the shape of the tracing cloud is largely affected by variations in velocity in the channel. Taylor (1954) suggested that the transverse shear rate and cross-mixing become equilibrated after a certain time scale at some point downstream. Beyond this point, the Fickian scattering equation can be used to model the tracing cloud concentration.

Proper management of the water body during the accidental spill of contaminants requires knowledge of the travel time, dispersion and maximum concentrations of contaminants in this channel. The mixing of pollutants in the water body and its transport has lead to a deep study on dispersion.

Longitudinal dispersal is a complicated transport process that is highly reactive to hydrology, hydraulics and changes in vegetation characteristics. Since vegetation is ubiquitous in all flood plains, their presence affects the transport of contaminants in these water bodies. Generally, vegetation in floodplains in rivers or in wetlands is a heterogeneous combination of grasses, shrubs and trees that influence sediment, nutrients and transport of pollutants. In addition, the vegetation present in a given body of water may be rigid, flexible or mixed, either in a submerged state or partially submerged. Vegetation presented either in natural river flood plains or in wetlands is recognized for their ability to improve water quality by filtering and diluting pollutants in different processes and can also modify the dispersal process Transport of contaminants. Vegetation can affect the longitudinal dispersal coefficient in rivers up to 70-100% compared with the non-vegetation case.

The study of dispersion downstream of vegetation can be useful to facilitate the requirement of pre-treatment or mass dilution of contaminants prior to their release into large bodies of water, thus causing a minimal effect on aquatic life.

Therefore, the present study aims to analyse the special distributions between two different sampling stations downstream of the vegetation when the dye is injected upstream into the vegetation. The objective of the experimental analysis will be to investigate the effect of vegetation on the longitudinal dispersion of the pollutant downstream of the rigid vegetation in a channel flow regime.

Throughout this study, natural flows were treated as exactly uniform, so that cross-sectional data would apply to cross-sections. The hypothesis may be misleading, but seems to give adequate results. The reason seems to be that in most flows, or at least in the one studied, it is possible to identify a characteristic cross-section which, although not identical to that of another, has a depth, a width and a typical distribution of speed. Since the tracer downstream of the current has an average of the effects of all cross-sections, the data of a typical section appear to suffice.

However, a more thorough study of the effects of non-uniformity in the chain is clearly justified. However, it was necessary to divide the flows into two classes: those in which the vertical the variations predominate, a limited class of very wide flows with few lateral variations; And those in which the lateral variations predominate, a class that includes most natural flows.

Even for the study of the fluxes in which the lateral variations predominate clearly, knowledge of the magnitude of the lateral mixing coefficient is at present scarcely adequate. The result was found to be adequate in these experiments, but there is no guarantee that it will be correct in other flows or types of laboratory flows. Probably the most important requirement for a future study is the identification of factors that control the rate of lateral mixing.

Although the method of predicting the dispersion coefficient for a natural flow was verified by numerous laboratory experiments and experiments in a natural flow. The analysis of the dispersion characteristics in the open channel flows was presented using the data collected by experimentation in this study and the data available from the studies of the previous investigators. “It was shown through analysis of the field and laboratory data that the dispersion coefficient (DL) value for the uniform flows remains constant with the distance whereas in the non-uniform flows DL varies with the hydraulic parameters”. It has been found that the DL value decreases with distance when the shear rate decreases in the direction of flow and has been found to increase with distance when the shear rate increases in the direction of flow.

1.2.1 Benefits of Longitudinal Dispersion

Given the growing demand on the nation's water resources, it is becoming increasingly imperative to apply rational criteria to the problem of allocating available water among competing uses. As the requirements increase, the allowable margin of error decreases. Too often, the information needed to make rational decisions is lacking.

An example of this problem is the use of streams and rivers as channels for the disposal of industrial, agricultural and domestic waste. Waterways have traditionally played this role. However, if pollution is not controlled, the availability of water for other uses can be greatly reduced. To combat pollution, the release of potentially hazardous contaminants in waterways must be regulated so that the flow capacity to maintain the concentration of contaminants within the allowed limits is not exceeded. This regulation requires knowledge of the rates at which flux systems are capable of transporting and dispersing contaminants. In general, rates of transport and dispersion depend on the physical and chemical nature of the contaminant, as well as the physiographic characteristics and the discharge in the stream system. However, the relationships between these factors and the transport and dispersal processes are extremely complex. Due to insufficient understanding of relationships and processes, the criteria for forecasting transport and dispersal rates are often unreliable.

With the introduction of the new generation of pesticides and agricultural herbicides, the need to improve the criteria for forecasting transport and dispersal rates has become more acute.

This is largely because many of these contaminants (1) have a tolerance level several orders of magnitude lower than most other pollutants, (2) are chemically very stable and retain their toxicity for long periods before yielding to natural or (3) cannot be eliminated by conventional water treatment practices.

1.3 Regression Analysis using SPSS Statistics

SPSS (Statistical Package for the Social Sciences) statistics is an IBM developed software package of Java platform used for logical batched and non-batched statistical analysis. Regression analysis is a statistical technique that is used to predict the variable of interest (known as dependent variable, criterion or target, the outcome) from a set of other variables (known as independent variables, regressor or explanatory variables, the predictor). Generally, a regression analysis

having two or more independent variables is called as multiple regression analysis. Regression analysis can be used for forecasting and prediction of various models. The results of regression analysis also help in depicting the independent variable which has major effect on the value of dependent variable. Checking R-squared value of the model is most common way of deciding its reliability. Also, the *p*-value obtained by the ANOVA table can be used for determining the significance of generated models.

Multiple linear regression is used for developing a correlation between D_L and independent parameter such as velocity, depth, density of rigid vegetation and U^*. Data to be used for the regression analysis, is to be obtained from work done in laboratory of various different configuration and discharge in ours experiment. And new equation of D_L is made using my analysis of longitudinal dispersion of rigid vegetation.

1.4 Objective of Thesis

Experimental study of the effects of different parameters on the longitudinal hydrodynamic dispersion coefficients for rigid vegetation having different configurations.

To develop a new equation of longitudinal dispersion coefficient through the rigid vegetation in channel flow considering the various parameters and validate the equation the experimental results.

1.5 Outline of thesis

The thesis comprises of seven chapters starting with the present one which through light on introduction to longitudinal dispersion, their benefits and regression analysis. The second chapter includes the literature review of the work done on the lateral and longitudinal hydrodynamic dispersion through rigid and flexible vegetation Chapter three deals with experimental programme which includes materials, tests conducted and procedure adopted for the experimental study. Chapter four includes the experimental data of the hydraulic as well as using tracer. Chapter five has all the results and findings of the experimental programme. Further, the comparison of predicted and observed values are also included in this and new equation of D_L on longitudinal dispersion of rigid vegetation also included in this chapter. Chapter six sums up the results obtained and their discussion followed by the conclusion.

CHAPTER 2

LITERATURE REVIEW

2.1 Literature review on lateral and longitudinal hydrodynamic dispersion through rigid and flexible vegetation

Agunwamba *et al* (1997) conducted a research on a laboratory to compare existing methods of collected tracer data. These methods include two-point sampling, where the inlet and outlet are sampled simultaneously at specific time (Levenspiel & Smith, 1957) until the tracer flows out completely. In addition, sampling is done from outlet to inlet which is the reverse in existing methods in literature. In achieving this, 60 g of salt was premixed and poured into a 14m channel and the concentration salt was measured and time concentration graph produced.

Result from both methods were compared and it showed that the former method gave underestimated values of dispersion coefficient which ranged from 0.9 to 3.3. Furthermore, the method seems to reduce cost, work and time used during tracer experiment. Consequently, this has been one of the major reasons why most researchers have resorted to laboratory and computer simulations in predicting dispersion coefficient values. This method has not been practiced in a river for validation.

Nepf *et al* (1997) conducted laboratory experiments to study the influence of vegetation on longitudinal dispersion and conducted that the mechanical dispersion increases as the population density increases but diffusivity within the vegetated system is consistently less than in the equivalent un- vegetated system due to the decrease in eddy scale caused by the presence of vegetation. Their results confirm that the presence of vegetation affects the longitudinal dispersion coefficient within the vegetation but the effect of vegetation on dispersion coefficient downstream has not been studied. Their experimental set up consisted the injection of rhodamine either upstream to the vegetation or at the centre of vegetation and detention time, resident time and spatial distribution were analysed by sampling either at the exit or one at entrance and other at exit.

Ahmad *et al* (1999) did laboratory experiments on longitudinal dispersion in clear-water open channel flows are reported. Analysis of laboratory and field data indicate that the dispersion coefficient is invariant along the length in uniform flows and varies with distance in non-uniform flows. Available predictors for dispersion coefficient are found not to yield realistic value of dispersion coefficient. As such, a new predictor for estimating the dispersion coefficient is proposed in this paper. The temporal variation of pollutant concentration computed using predicted DL value and a numerical scheme previously developed by the authors showed good agreement with the observed temporal variations. In non-uniform flows the value of dispersion coefficient varies with distance due to varying values of hydraulic parameters.

Agunwamba *et al* (2002) in his study discussed about the subjective nature of sampling time and intervals indulged by various researchers during tracer studies. At will, some select intervals and periods which differs from one another. In his study, the precision, confidence and design efficiency of tracer experiment in the estimation of dispersion coefficient and velocity were investigated. This was achieved with data from a laboratory study (Agunwamba, 1997) and a field work executed in Portugal (Marecos do Monte & Mara, 1987). The study revealed that it is possible to predict proper sampling procedures before experimental process takes place and indulging in large number of experimental runs may not yield precision in experiments. Obviously, this would have led to more energy, time and money expended. Furthermore, he suggested that more time should be spent to determine the apex of the breakthrough curve (BTC) than the tail for efficient determination of dispersion coefficients.

Serra *et al* (2004) carried out an experimental investigation to quantify the effect of randomly distributed emergent vegetation on lateral diffusivity as a function of the plant diameter, distance between them, flow velocity and the drag coefficient. The analysis is made for very low Reynolds number ranging from 10-90 and study has not been done foe higher Reynolds number. Their experimental set up consisted of the injecting rhodamine at entry to the vegetation and the concentration distribution in the vegetated zone was obtained and developed a new model for longitudinal dispersion in channels with submerged vegetation and validated the model with experimental results.

Napiórkowski *et al* (2004) conducted a research on numerical computations are presented for the longitudinal transport of passive, conservative solutes in an actual river channel with the inclusion of its geometrical complexities. Only one-dimensional conditions after a substance has become fully mixed across the depth and width of the river are concerned. Two different situations are considered, namely a linear version in which one can assume that the mean velocity does not vary along the channel course and when the model parameters are constant and the nonlinear version implying channel nonuniformity (and variability of model parameters along the channel). The results of tracer tests carried out in the selected reach of the Wkra river in Central Poland have been used in the analyses. A model taking into account the changes of model parameters along river channel proved to provide better results when compared to the experimental data but the parameter identification in such case is computationally much more expensive. In the study, a special procedure was designed for the identification of the parameters of the model of longitudinal transport of pollutants in rivers with the inclusion of the phenomenon of transient storage. A model taking into account the changes of model parameters along river channel proved to provide better results when compared to the experimental data but the parameter identification in such case is computationally much more expensive.

Nepf et al (2007) defined vegetation is ubiquitous in rivers, estuaries, and wetlands, strongly influencing water conveyance and mass transport. The plant canopy affects mean and turbulent flow structure, and thus both advection and dispersion. Accurate prediction for the transport of nutrients, microbes, dissolved oxygen and other scalars depends on our ability to quantify the impact of vegetation. In this paper, we focus on longitudinal dispersion, which traditionally has been modeled in vegetated channels by drawing analogy to rough boundary layers. This approach is inappropriate in many cases, as the vegetation provides a significant dead zone, which may trap scalars and augment dispersion. The dead zone process is not captured in the rough boundary model. The canopy density was varied between $ad = 0.015$ and $ad = 0.048$, within a range representative of field conditions, as cited by Ghisalberti and Nepf (2004). Velocity profiles for runs were measured by acoustic Doppler velocimeters, as reported in Ghisalberti and Nepf (2004). For the remaining runs, velocity measurements were taken by a two-dimensional (2D) laser Doppler velocimeter (LDV). A 300mW blue-green argon-ion laser was used in conjunction with a Dantec 58N40 flow velocity analyzer (FVA) unit. Experimental runs were terminated when tracer mass in the leading edge of the cloud, had recirculated around the flume. Each condition

was repeated five times. For several cases, the fluorometer was positioned at three different lateral locations for the same flow condition. The difference in dispersion coefficient obtained at each location was within the uncertainty of the method, demonstrating that a single measure at midwatch was sufficient.

Hunta *et al* (2008) predict the transport of non-sorbing solutes through water flow in the subsurface. He derive the first reliable calculations of the entire distribution of arrival times, for nonsorbing solutes in adjective flow in strongly disordered porous media. It generates longitudinal dispersion (in the direction of flow) in the absence of diffusion. The results are found to be predictive when compared with simulations of two-dimensional flow on percolation structures, and appear to have relevance for experiments as well. The calculated W(t) appears to generate quantitatively accurate predictions for appropriate simulations as well as results in general accord with experiment. The long-time tail of the arrival time distribution may, in some cases, be consistent with Gaussian spreading of solute plumes, but more frequently with an approximate power-law decay. The calculations are based on a synthesis of critical path analysis (from percolation theory) and scaling arguments (also from percolation theory). Further theoretical development to account for arbitrary saturation is necessary. We require further numerical development as well to produce a spatial distribution of contaminants at time t. Such a development would allow comparison with a wide variety of additional experiments for which results are reported as longitudinal dispersion coefficients.

Baek *et al* (2010) proposed a modified version of the routing procedure (RP) model. The model sort to take care of irregularities that abound in a river environment which includes presence of meanders and transient zones. The new model is a mix of channel geometry, advection equation and steam tube concept. Tracer data was obtained from a field study in natural rivers in Korea

having range of 1.3–1.9 km in length and intervals of 200–400 m. With the data collected, the new model was calibrated and when tested gave values close to other methods. The unique thing is that the model was able to capture the irregularities such as bends and straight zones as high and low concentration values were obtained at those points when even measured.

Singh et al (2010) conducted laboratory experiments on a rectangular open channel on passive mixing of pollutants in longitudinal and vertical directions due to a transverse line source on the flow surface are reported. Laboratory experiments on passive mixing of pollutants in open channels with transverse line slug source on the flow surface were conducted. The finite difference scheme recently proposed by the authors for the prediction of pollutant concentration was extended to determine the optimum (observed) values of the mixing coefficients from the observed concentration versus time curves. The computed vertical mixing coefficient from an empirical equation and from the measured velocity distribution were compared with the optimum using the data of the present study and these collected from the literature. In both cases, most of the computed values lie within a scatter band of 50–100% times of the observed data. The errors, likely to occur in the predictions of the concentration versus time curves due to the use of the erroneous values of longitudinal and vertical mixing are quantified, indicating that the predictions of concentration versus time curves can be made with a maximum error of about +30% if about +100% error is contained in the values of longitudinal and vertical mixing coefficients. Based on the computational results, a constant longitudinal mixing coefficient equal to longitudinal dispersion coefficient of a 1D dispersion process is recommended for practice, rather than a variable value along the flow depth.

Shucksmith *et al* (2011) prediction of the physical transport and mixing of pollutants or other soluble material is crucial for effective river management. Although well-established methods exist which describe mixing processes in open channel flow, the presence of vegetation has a significant impact on mixing and few existing techniques account for this. To date, existing models which predict longitudinal dispersion coefficients in vegetated open channel flow have been derived and verified based on experiments conducted in simulated vegetation. This paper presents observations of longitudinal dispersion coefficients in a channel featuring living vegetation and tests against both an existing and a newly proposed model for longitudinal dispersion coefficient in submerged vegetated open channel flow. A model based on a mathematical technique of predicting dispersion in plain shear flow is shown to be capable of predicting longitudinal dispersion coefficients to within 20%.

Open channel flows with submerged vegetation are complex mixing systems, involving different flow layers (wake, mixing, and free flow layers). The rate of mixing in such systems is dependent

on the relative size of the flow layers, the difference in average velocity, and the rate of transfer of mass between the layers. Of these expected influential parameters, the most difficult to predict is the size of the mixing layer; which was found to be approximately constant in growth phase Carex, but to be substantially larger in the cropped Carex. A method for predicting mixing layer depth derived by Nepf et al (2007).

Kim *et al* (2011) explored the use of radioisotopes for the determination of dispersion coefficient in Daejong river located in south eastern Korea. The radioisotope had limited life span; therefore, it was injected twice in a day (morning and evening) into the river which had width and depth range values of 18–30 and 0.2–20 m respectively. With two points marked downstream, the varying concentrations of the tracer was detected using a 2 × 2 in. NaI(TI) scintillator detector which was placed stationary at the two points downstream. The work confirmed that the concentration values that were calculated agrees with the measured when statistically compared.

Albuquerque *et al* (2012) evaluate of the dispersion in vegetated beds may allow identifying mechanisms that affect the transport and reaction of solutes, namely organic and nitrogen compounds. A set of non-reactive tracer experiments (slag injection) was performed in a vegetated bed used for the removal of organic and nitrogen pollutant loads. Loads of approximately 300 mg COD/L and 30 mg NH4-N/Land a hydraulic loading rate of 3.5 cm/d were used. The results showed a delay in all the residence time distribution (RTD) curves and a variation in the dimensionless residence time curves, which means that the mass center of the impulse was late relatively to the expected one. An analytical solution of the Multiple-Tanks-in-Series (MTS) model well represents the RTD curves obtained in the tracer experiments. The detected dispersion and dead volume ratios (7% to 12%) did not affect the performance of the bed, which presented mean removal efficiencies of 85% and 60.4% for COD and NH4-N, respectively. The results show that there was a delay in the tracer exit in all the bed's sections, which may have been related to the presence of stagnated areas and the occurrence of internal recirculation, due to the development of clusters of biomass, roots, rhizomes and solid material. However, those conditions seem to have not interfered with the treatment performance of the Filtralite-based HSSF beds, which presented a high removal of COD and NH4-N, one year after the start-up.

Agunwamba *et al* (2013) in their experiment on tracer studies compared dispersion coefficient values obtained in a natural stream by using a relatively new Euler-Lagrangian model, Fisher's model and Levenspiel and Smith models or approach. It was achieved by extracting stream data from American stream tracer analysis (ASTA) on the Humboldt river as well as performing tracer studies in a river in Ebere, Enugu state, Nigeria. 50 kg of salt was pre-mixed and then poured in the river that was 2.5 km long having spacing of 200 m. Consequently, variable distance constant time method of sampling was employed and taken to the laboratory for analysis. Computation of dispersion coefficients were done using the mentioned three approaches. Results showed that slightly increased values of dispersion were obtained from Agunwamba model than in Fisher's while larger values were obtained in Levenspiel and Smith model. Although Agunwamba's approach was observed to take for taking more time during computation than the others, it was commended for requiring less data input, labour input and cost.

Zeng. H. *et al* (2014) obtained the LD from a set of 116 tracer data. This data was obtained from over 50 rivers sited in the United Kingdom (UK) and the United State (US). Comparisons were made as performance of ten frequently used model in literature were varied seeking precision. The rivers generally had aspect ratio between 20 and 100. Again, results from the work showed that the LD coefficient values were underestimated for any given value of aspect ratio. Zeng and Huai (2014) developed a model which is an upscale of the models commonly used for LD coefficient estimation. This new model even though may not be suitable for estimation of dispersion coefficient in a rectangular flume but is very efficient in predicting LD in streams or rivers having trapezoidal sections not having width (B) <15 m and >259 m. In concluding, he affirmed that LD coefficient has a strong tie with the product of depth of river (H) and cross sectional velocity (U) than HUx, Ux is the shear velocity.This is in accordance with many researchers as tracer concentrations are obtained at different measuring points as velocity variation brings about mixing process. This is against earlier method carried out by Levenspiel and Smith approach (Agunwamba, 1997).

Camenen *et al* (2014) objective of this article is to investigate the major issues associated with the calibration of the pollutant dispersion in 1-D hydraulic models applied to river networks, especially large, complex, artificialized ones where ecological and socio-economical threats are important. Experimental dispersion values were quantified using both the change of moment method and a

simple fit-by-eye procedure for eight rivers reaches with homogeneous hydraulic conditions and an achieved tracer mixing and dispersive equilibrium. Since dispersion coefficient values depend on the assumed dispersion model, ideally, they should be calibrated using the same model in which they are to be used, as was done in this study. It appears that the formulae for which the fit was mainly based on the cross-sectional aspect ratio are generally more appropriate for field data than those which are sensitive to the velocity to shear velocity ratio. Implementing them in 1-D river models is still an interesting research perspective. An important issue is that calibration fits that account for transient storage effects may provide significantly different values for the Fickian longitudinal dispersion coefficient. This observation reminds us again that dispersion coefficient values depend on the simulation method used, and that ideally, they should be calibrated using the same model in which they are to be used, as was done in this study. So far, introducing transient storage in 1-D hydraulic models might be a negligible improvement, in case the mainstream longitudinal dispersion coefficient is not parameterized accurately based on an appropriate predictive formula.

Abderrezzak *et al* (2015) conducted a research comparing the extent to which LD empirical formula can be used in 1-D numerical modelling (Mascaret tool). This was actualized by conducting eight laboratories experimental study using Rhodamine WT as tracer. The varying concentration values were obtained at four stations downstream of a 30m length channel using a Turner fluorimeter. Furthermore, the assessment was done comparing with Ten empirical formula existing in literature with regards the shape of their BTC's. The result showed that of the ten empirical models assessed, Iwasa and Aya (1991) with Seo and Cheong (1998) were better predictors when compared to the 1-D numerical modelling tool used by Abderrezzak et al. (2015). Therefore, their model could be employed for dispersion coefficient prediction in streams having same in-stream (width, flow, depth, meanders, amongst others) properties. On the other hand, Elder (1959), Fischer (1975) and Iwasa and Aya (1991) were better off for laboratory scale dispersion coefficient prediction. In conclusion, it was suggested that the models that performed well and models frequently used should be adjusted to fit complex geometry having transient storage conditions which are likely situations of many rivers. This will surely increase the model applicability.

Meddah *et al* (2015) proposed the use of a 1-D Transmission Line Matrix(TLM) method for estimation of LD coefficient. This came to light as it could save time for mathematical computation and less data input. This was verified by simulating and comparing with a data-set obtained from a River Severn based in UK. Rhodamine WT was used as tracer in a 14km long river the result used was culled from a study carried out by Atkinson and Davis (2000). From the study, it was gathered that the model overestimated flow velocities and LD coefficients but describes well peak concentrations as time progresses. The latter is good as peak concentrations appears to be an important finding during tracer studies (Agunwamba, 2002). However, the assumptions and governing principles of the model, which are not completely true of a typical river or stream, make regular tracer data collection of streams that are prone to pollution paramount.

Parsaie *et al* (2015) study on the mechanism of Pollutant transmission in the river is a major part of the knowledge of environmental engineering. If the pollution transmission mechanisms in the river with various geometries were specified, the river water quality managing does by more accuracy and his leads to reduce the effects of river pollution on public human's health. In this paper, the pollution longitudinal dispersion coefficient (LDC) is calculated by dispersion routing method for Severn River. They considered seven stations along the river for measuring and record the concentration profile at each station. For calculating the LDC by empirical formulas, 12 of the famous equations related to the dispersion coefficient is collected and assessing them to calculate the LDC for Severn River shows that the Tavakollizadeh and Kashefipour equation by correlation coefficient about 0.4 is the most accurate empirical formula. The Dispersion routing method is a suitable method to calculate the dispersion coefficient in rivers by using the tracer profile concentration. The results of this study show that using the empirical formulas for calculating the dispersion coefficient in Severn River includes incredible and result of them is inappropriate for the river water quality management; so, conducting the field studies is unavoidable.

Abderrezzak *et al* (2015) one-dimensional (1-D) numerical models of solute transport in streams rely on the advection–dispersion equation, in which the longitudinal dispersion coefficient is an unknown parameter to be calibrated. In this work, we investigate the extent to which existing empirical formulations of longitudinal dispersion coefficient can be used in 1-D numerical modelling tools of solute transport under steady and unsteady flow conditions. Ten empirical formulas of longitudinal dispersion coefficient are then tested by simulating eight laboratories

experimental cases under steady flow condition and the solute transport. The objective of this paper was to investigate the major issues associated with the calibration of longitudinal dispersion coefficient in numerical modelling of solute transport in streams. This analysis represents a new step forward assessing the applicability of dispersion coefficient formulations in numerical studies. Based on criteria involving the peak concentration and its arrival time at various locations, predictors for the entire range of conditions of the experiments. For the entire range of conditions studied in this work, we recommend the longitudinal dispersion coefficient formula proposed by Iwasa and Aya (1991). Evaluation of the performance of the selected formulas should be extended to other cases with complex geometry (floodplains, transient storage zones) and reactive pollutants. This is the next phase of this research and results will be reported in the future.

Singh *et al* (2015) conducted a research on analytical method to developed the longitudinal dispersion coefficient in Fischer's triple integral expression for natural rivers. The method is based on the hydraulic geometry relationship for stable rivers and on the assumption that the uniform-flow formula is valid for local depth-averaged variables. The suggested expression for the transverse mixing coefficient equation and the direct integration of Fischer's triple integral are employed to determine a new theoretical equation for the longitudinal dispersion coefficient. By comparing with 73 sets of field data and the equations proposed by other investigators, it is shown that the derived equation containing the improved transverse mixing coefficient predicts the longitudinal dispersion coefficient of natural rivers more accurately. The prediction of the longitudinal dispersion coefficient in ice-covered rivers was relatively accurate, since the flow was nearly uniform by being restricted in the main channels. Therefore, the proposed analytical expression could be a good tool to estimate the longitudinal dispersion in ice-covered rivers. Using the hydraulic geometry relationship of stable rivers, a channel shape equation or a transverse profile equation of local flow depth is derived. Using the suggested equation for the transverse mixing coefficient and the direct integration of Fischer's triple integral, a new equation for the longitudinal dispersion coefficient for natural rivers is derived by taking into account the irregularity of natural rivers. By comparing with 73 sets of field data and the equations proposed by other investigators, it is found that the new has the least error in predicting the longitudinal dispersion coefficients for natural rivers. More than 64% of the predictions by the new equation fall within the range of $0.5 < K_{prediction}/K_{measurement} < 2$. Moreover, as compared with

existing equations, the new equation is theoretically based, more accurate, and clarifies its dispersion mechanism. The future investigation into longitudinal dispersion should highlight the determination of an accurate transverse dispersion coefficient equation and the influence of channel irregularity.

Zaramella *et al* (2015) proved solute transport in rivers is controlled by surface flow hydrodynamics and by transient storage in dead zones, pockets of vegetation and hyporheic sediments where mass exchange and retention are governed by complex mechanisms. The physics of these processes are generally investigated by optimization of transient storage models (TSMs) to experimental data often yielding inconsistent and equifinal parameter sets. Uncertainty on parameters estimation is found to depend not only on the rates of exchange between the stream and storage zones, the stream-water velocity and the stream reach length according to the experimental Damkohler number (DaI), but also on the relative significance between transient storage and longitudinal dispersion on breakthrough curves (BTCs). An optimization strategy was developed and applied to an experimental dataset obtained from tracer tests in a small lowland river, analyzing BTCs generated through tracer injections under different conditions. In particular, when the experimental Damkohler number increases, transient storage and longitudinal dispersion become competing mixing processes and their signatures overlap yielding equifinal and uncertain parameter sets. Parameters were estimated according to an analysis of their relative significance, based on the relative importance of model sensitivity. The estimated longitudinal dispersion coefficient yielded a value close to $DL / HU\hat{} * = 5.93$. Similarly, the transient storage components were estimated from the rest of the BTC, were fast and slow exchange signatures resulted to dominate over longitudinal dispersion. Using this method, transport and storage parameters of a double compartment TSM were consistently estimated.

Seoa *et al* (2016) analyzed of two-dimensional pollutant mixing i.e. lateral and longitudinal is necessary for the effective water quality management in natural streams. In this study, numerical simulations were performed to predict the 2D pollutant behavior, using the FEM-based river analysis software, RAMS. Pollution propagation was estimated by the 2D advection-dispersion model, CTM-2D. Velocity field was computed by the 2D shallow water model, HDM-2D. Dispersion coefficients are key input parameters in CTM-2D. To calibrate these parameters, tracer tests using Rhodamine-WT dye solution were conducted in the Sum River, Korea. The calibrated

longitudinal dispersion coefficients from field studies showed values about 6 times larger than the theoretical from the Elder's equation (Fischer, 1967) about 6 times larger than that from the Elder's equation, $DL / HU^* = 5.93$ (Fischer, 1967). In the meandering channel, the recirculation zone and secondary current capture the tracers to yield the transient-storage effect in the C-T curve. Therefore, the dispersion stress in the momentum equation should be essential to efficiently investigate the 2D pollutant mixing in rivers with complex geometry and flow field.

Wenxin et al (June 2016) defined suspended canopies can cause flow disturbances such as reducing velocities within the canopy, and increasing flow beneath the canopy. Flow modifications by canopies dramatically affect the fate and transport of sediment, nutrients, contaminants, dissolved oxygen, and fauna in aquatic systems. A three-zone model is presented here to predict the longitudinal dispersion coefficient by simplifying Chikwendu's N-zone model. To validate the model, both flow field and tracer experiments were conducted using a straight rectangular Plexiglas flume, with rigid circular rods as the modeled suspended canopies. The result shows that velocities increased above the flume bed and maximized at a point between the canopies and flume bed. Above that point, stream wise velocities decreased into and within the canopies. Reynolds shear stresses were largest at the canopy interface and smallest (zero) at the velocity maximum point. Good agreement between the modeled results and experimental data shows that the model can effectively predict the longitudinal dispersion coefficient in open channels with suspended canopy. Aquatic vegetation is ubiquitous in natural rivers. Equations of longitudinal dispersion in open channels, which generally assume a logarithmic velocity profile, cannot be directly applied to vegetated channels, so traditional equations of longitudinal dispersion in open channels cannot be directly applied to vegetated ones. Aquatic vegetation is usually classified as emergent, submerged, or suspended. In contrast with the other two types, suspended vegetation extends downward from the water surface rather than upward from the bed (Plew et al.2006). Field observations have shown that suspended canopies can cause flow disturbances such as reduced velocities within the canopy, and increased flow beneath the canopy.

Suraya et al (2016) looks into the flow profiles in terms of longitudinal and transverse velocities, turbulence intensity and turbulent kinetic energy in relation to the vegetation density, flow depth and stem Reynolds number. An experimental study was conducted in a fully vegetated flume,

whereby a control volume was selected for detailed velocity measurement using Acoustic Doppler Velocimeter (ADV). This research considered 0.97%, 3.90% and 7.80% vegetation density or solid volume fractions (SVF) which are categorized as sparse in the lab work. Series of experiments were conducted in uniform flow condition with stem Reynolds number, Red ranging between 1300 and 3000. Experimental results managed to capture the wake area and fast flow region. The boundary between the wake area and fast flow region is reflected by the highest magnitude of the normalized longitudinal turbulence intensity and turbulent kinetic energy. Positive normalized transverse velocity represents the flow diversion away from the vegetation and the negative normalized transverse velocity indicates flux towards the centre of the wake. The analysis shows that normalized longitudinal velocity reduces around 50% as the vegetation density doubles and shallow water depth generates greater flow resistance compared to high water depth. Further analysis reveals that the negative transverse velocities dominate in aligned vegetation and positive transverse velocities dominate in staggered vegetation. Positive transverse velocity represents the flow diversion away from the vegetation and the negative transverse velocity indicates the flux of flows toward the centre of the wake. Normalized longitudinal turbulence intensity displays the highest magnitude at the wake edge. Also, the normalized longitudinal turbulence intensity presents a negative trend with the stem Reynolds number which indicates lower magnitude of turbulence in the fast-flowing region. This is similar to the turbulent kinetic energy that is lowest at the fast flow region located at the centre of the control volume. Meanwhile, the magnitude of the turbulent kinetic energy increases in the wake area downstream the vegetation. To conclude the present experimental study manages to capture the wake area (velocity deficit zone) and the fast flow region.

Yongcan, C. *et al* (2016) considered the ice-cover effects on the longitudinal dispersion coefficient in rivers. The dispersion coefficients due to either the vertical or transverse velocity shear are calculated using Elder's or Fisher's triple integral equation, respectively, based on the assumptions of a parabolic cross section and a vertical logarithmic velocity distribution in both the riverbed and the ice-cover zones. The results show that in ice-covered natural rivers, where the aspect ratio is usually larger than 10, the dispersion coefficient due to the transverse velocity shear is 50 times greater than that due to the vertical velocity shear. An analytical formula for longitudinal dispersion coefficient is further developed by the simplification of Fischer's triple integral

equation, and it is validated against field tracer tests with discrepancy between observations and predictions less than 150%. Comparing the proposed formula to the most widely-used Fischer's formula demonstrates that for wide and shallow rivers the presence of ice-cover will lead to about a three-fold increase in the magnitude of the longitudinal dispersion.

Bressan *et al* (2016) conducted a research on the issue of water pollution has worsened in recent times due to releases, intentional or not, of pollutants in natural water bodies. This causes several studies about the distribution of pollutants are carried out. The water quality models have been developed and widely used today as a preventative tool, i.e. to try to predict what will be the concentration distribution of constituent along a body of water in spatial and temporal scale. To understand and use such models, it is necessary to know some concepts of hydraulic high on their application, including the longitudinal dispersion coefficient. This study aims to conduct a theoretical and experimental study of the channel dispersion coefficient, yielding more information about their direct determination in the literature. The results showed that there was dispersion of the initial concentration of NaCl spatially and temporally, based on data found for the coefficient at each point.

CHAPTER 3

EXPERIMENTAL APPARTUS AND TECHNIQUES

3.1 DESCRIPTION OF EXPERIMENT

Experiment were made on open channel having dimensions 0.7m wide, 0.6 m deep and 6m long located outside water resource laboratory of our Institute as shown in figure 3.1.

The objective of this experiment was to measure the effect of different parameters on longitudinal hydrodynamic dispersion coefficient for rigid vegetation having different configuration. The experiment set up consisted of a graduated dropping funnel having a knob, containing rhodamine WT as a tracer of some concentration (10000 ppb), fixed at 1m away from one end of channel. The acrylic tubes of diameter 12, 16 and 20mm are used as a rigid vegetation and fixed on a sheet having dimension 800x600mm with different configuration. The acrylic tubes are kept in channel as partially submerged at distance of 2m from point of injection. The collection point of sample of water are taken at distance 1m, before and after the vegetation and at 4m from point of injection. Experiment were conducted for different configuration of vegetation with different diameter and having varying spacing between the acrylic tube. Figure3.1 shows the schematic arrangement of cylinders where the tubes are placed in staggered manner. The spacing between the tubes in a row is kept uniform and the spacing between two rows kept 10cm, 7.5cm and 5cm as well. The sample of water collected at 1m, pre-and post-vegetation and at 4m of the source of injection of tracer. The discharge is measured using the calibrated triangular v-notch fitted at the end of the channel. A trilogy lab fluorometer designed by Turner Design having minimum detection limit of 0.02 ppb of rhodamine WT was used to measure the concentration of tracer. Initially the rhodamine of 10000 ppb is prepared and 40 ml of tracer put in the graduated dropping funnel. The funnel is made empty at a time and sample of water collection at all four points are started at a fixed time interval immediately after the emptying of the funnel. The dye is released at the centre point of the channel keeping the funnel tip at the water surface as shown in figure 3.1. The concentration of rhodamine WT in various samples collected is measured using fluorometer. The water samples are collected upstream of the point of injection of rhodamine to check the background concentration of incoming water and no concentration of rhodamine is found during the experiment.

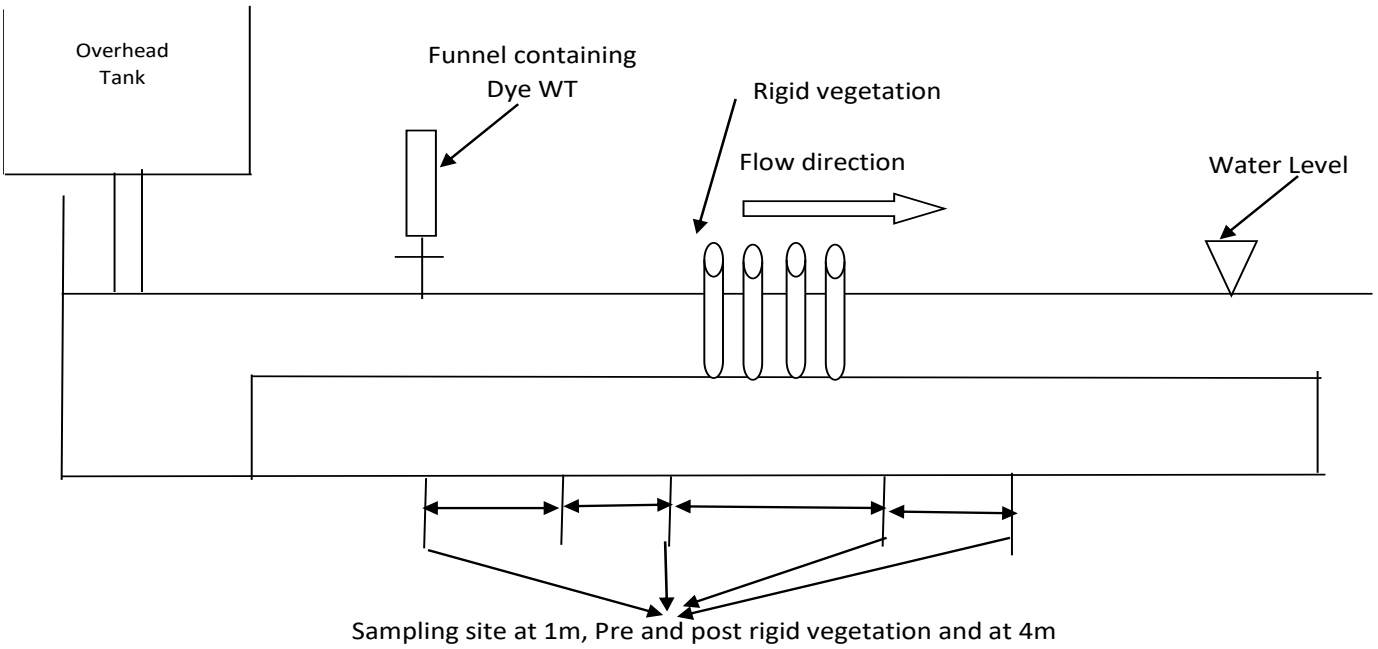

Figure 3.1 Schematic diagram of flume used in dispersion experiment

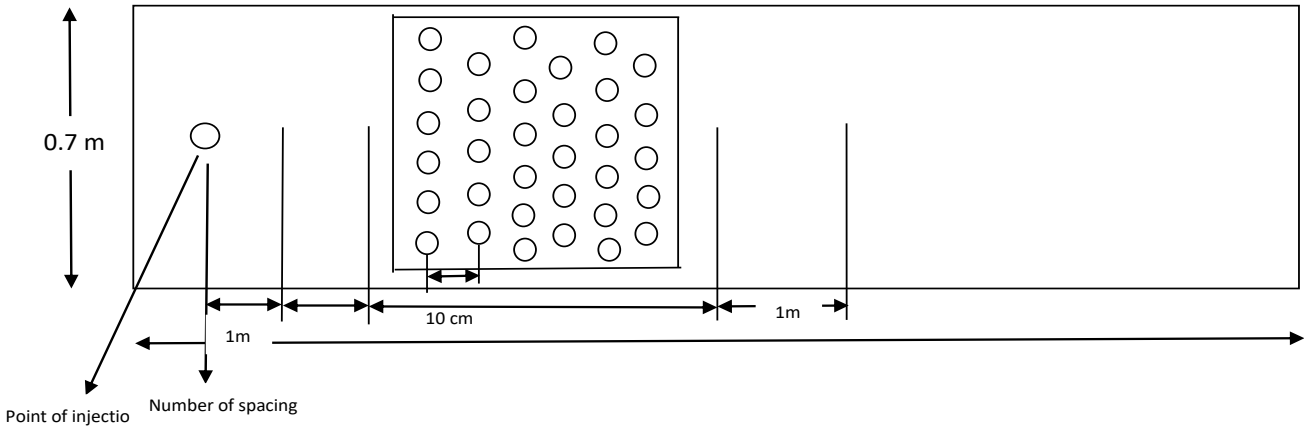

Figure 3.2 Arrangement of rigid vegetation in channel (plan view)

Figure 3.3 Detailed arrangement of rigid vegetations along with injection of rhodamine WT in a channel

Figure 3.3 shows the detailed arrangement of experiment taken during the experiment. The staggered arrangement of acrylic tubes is kept at distance 2m from injection point of tracers. The injection of tracer is made at the centre of the channel. The tracer was made to pass through the rigid vegetation and the collection of the water sample was made at the downstream of the vegetation. The sample collected was tested in trilogy lab fluorometer shown in figure 3.7 for the presence of tracer.

3.2 OPEN CHANNEL

Open channel flow is defined as fluid flow with a free surface open to the atmosphere. Examples include streams, rivers and culverts that do not flow completely. The open channel flow assumes that the pressure at the surface is constant and the hydraulic grade line is at the surface of the fluid.

3.2.1 Description. The experiment was conducted in a 6 m long and 0.7m wide open channel located outside the water resource lab Thapar University Patiala. The bottom of channel is made of concrete. And an instrument fastener railing is made on both side of channel. The channel is attached with an overhead tank of capacity 1 Lacs Litres. And the centrifugal pump is used to fill up of overhead tank and discharge is kept controlled with the help of a rotatory valve. Several small pits are made in between channel so that the water had minimum fluctuations. The water i.e. flowing through channel is directed to an underground tank and then again with the help of centrifugal pump raised towards overhead tank so that there is negligible wastage of water and same water is used again and again although the concentration of dye WT kept increasing as same water was used again but since it is of very small amount, therefore the effect was neglected.

Analysis of the flow patterns of the surface water form, velocity, shear stress and discharge through a stream flow falls under the Open Channel heading.

3.3 WATER DEPTH AND VELOCITY MEASURING EQUIPMENT

3.3.1 Triangular v-notch: Water depths in the flume measured with the pointer gage and which could be read to the nearest of 0.01cm was mounted on instrument carriage.

The discharge is measured with the help of V-notch which is at the end of channel and formula to measure discharge is shown in equation (*) below.

$$Q = \frac{8}{15} \times C_d \times \sqrt{2g} \times tan\frac{\theta}{2} \times H^{\frac{5}{2}} \qquad (*)$$

Where,

C_d = coefficient of discharge

g = acc. Due to gravity taken as 9.81 m/s^2

Θ = angle of v- notch taken as 90°

H = Depth measure at v-notch

And Q = discharge of channel in (m^3/s)

Figure 3.4 Open channel with instrument fastener

In our experiment, we calibrated the v-notch and measured C_d =0.72 and used C_d as 0.72 in all our discharge calculations. And we also calibrated our V-notch open channel with the help of ADV and found C_d nearly equal to 0.7.

3.4 Tracer

Rhodamine WT is a bright fluorescent red dye originally developed for water tracing applications. We used it in our experiment as a water tracer and also calibrated the fluorometer with the rhodamine dye. A trilogy lab fluorometer designed by Turner Design having minimum detection limit of 0.02 ppb of rhodamine WT is used to measure the concentration of tracer. Initially the rhodamine of 10000 ppb was prepared and 40 ml of tracer was put in the graduated dropping funnel. The initial concentration of dye was 10^9 ppb and by diluting it with distilled water solution of 10000 ppb was prepared. Rhodamine WT was used as a tracer because the specific gravity of both water and rhodamine is approximately equals (i.e. 1g/ml water specific gravity and 1.16 g/ml rhodamine specific gravity)

Figure 3.5 Rhodamine WT of 10000ppb in flask

3.5 FLUID SAMPLING APPARTUS

Water samples were taken out from channel with the help of small 10ml biles at 4 different location as shown earlier and approximately 50 samples were collected from the 1 sampling site with same time interval. These small biles were kept in acrylic rack number wise i.e. first bottle at one number and so on.

Figure 3.6 Sampling Biles of 10 ml each in acrylic rack

3.6 TRILOGY LABORATORY FLUOROMETER

The Trilogy Laboratory Fluorometer is a multifunctional laboratory instrument that can be used to perform fluorescence, absorbance and turbidity measurements using the appropriate optical module. A colour touch screen with simple menus allows an intuitive and user-friendly interface. Fluorescence modules are available for discrete sample measurements of various fluorescent materials, including chlorophyll, rhodamine, fluorescein, cyanobacterium pigments, ammonium, Optical brighteners, histamines, crude oil, hydrocarbons and other fluorescent compounds. The Absorbance module accepts interchangeable filter pallets so that measurements can be made at different wavelengths to identify or place a sample in a particular class of compounds. The wavelengths / bandwidth of the standard filter bar is: 560/10; 600/10 and 750/10 nm. The Turbidity module uses a green (IR) LED with a wavelength of 700nm "Water Quality - Determination of

Turbidity". Using infrared LEDs can measure turbidity at wavelengths that are not normally absorbed by organic matter, thereby reducing sensitivity to interference. The optical modules contain the light source and filters necessary for the application concerned.

Figure 3.7 Trilogy Laboratory Fluorometer

3.7 RIGID VEGETATION (ACRYLIC TUBES)

In our experiment, we used acrylic tubes as a rigid vegetation of three different diameter (12, 14 and 20mm) and with three different configurations (5cm, 7.5cm and 10cm c/c spacing). These rigid vegetations are fixed on a sheet having dimension 800x600mm with the help of quick fix as shown in figure 3.8.

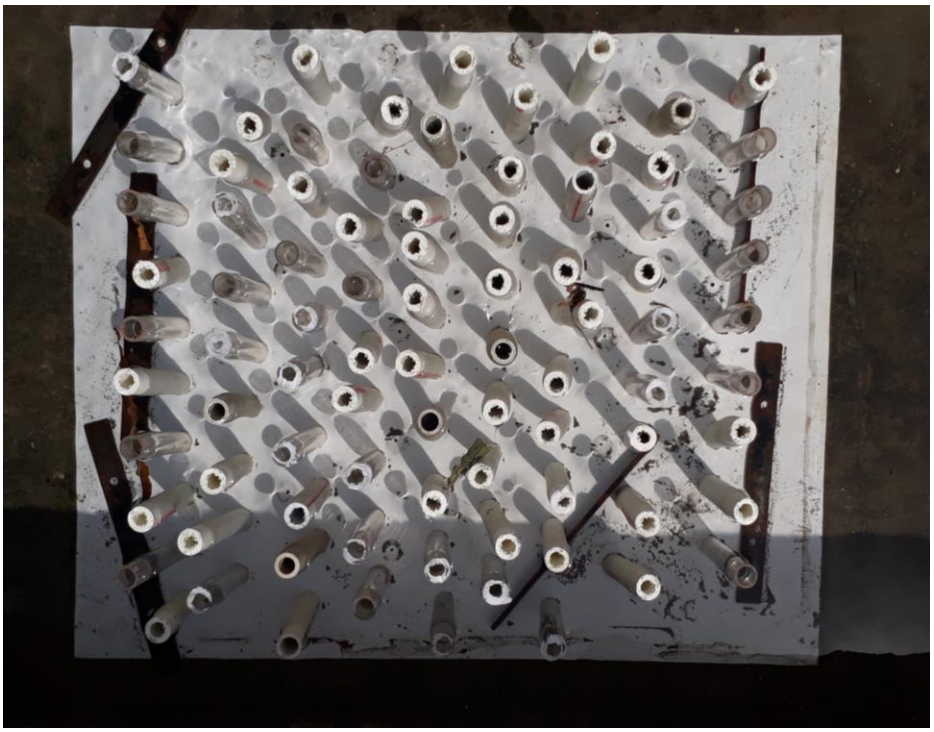

Figure 3.8 Rigid vegetation having dia. 20mm and 7.5 cm c/c spacing

These rigid vegetations are kept in channel at distance of 2m from point of injection and are kept partially submerged in water. By using one configuration of rigid vegetation we did three experiments by varying discharge value and measure the effect of vegetation on longitudinal dispersion.

3.8 SOFTWARE USED

In this study, Microsoft Fortran Power Station and IBM SPSS Statistics were used. Two programs were made in Fortran language, one was for Fischer Routing and other was for Dispersion. The

input is added with the help of notepad into the program and output is in the form of excel data. After getting D_L data from both program a comparison is made between them. The SPSS Statistics was used for linear regression analysis and an equation of D_L was made with the help of SPSS.

3.9 METHODOLOGY

The dispersion coefficient can be determined by the classical method based on the moments of concentration in which the variance of the tracer cloud increases linearly with time and can be expressed as shown below. The dispersion coefficient is determined by the momentum method using equation 3.1-3.5 given below.

$$\sigma_t = \frac{1}{2}\frac{d\sigma_x^2}{dt} \quad (3.1),$$

Where,

$d\sigma_x^2$ is the variance of the spatial variance of the longitudinal direction, equation 3.1 can be expressed in terms of the properties of the distribution of the temporal concentration on two longitudinal sites.

$$D_L = \left(\frac{U_C^2}{2}\left(\frac{\sigma_t^2(x_2)-\sigma_t^2(x_1)}{t_2-t_1}\right)\right. \quad (3.2),$$

Where U_C is the velocity of tracer cloud, σ_t^2 is the variance of the concentration-time curve, $t_2\ and\ t_1$ is the time of travel of the centroid of the concentration-time curve at upstream and downstream site respectively.

The velocity of tracer cloud can be expressed as

$$U_C = \frac{x_2-x_1}{t_2-t_1} \quad (3.3),$$

Where U_C is the velocity of tracer cloud, and t_1 and t_2 are the time of travel of the centroid of the concentration-time curve at u/s and d/s. The centroid of the concentration-time curve and temporal variance of a tracer wave (Day, 1975) at a particular site can be expressed as

$$t_c = \frac{\int C(t)tdt}{\int C(t)dt} \quad (3.4),$$

$$\sigma^2 = \int \frac{C(t)t^2 dt}{\int C(t)dt} - t_c^2 \quad (3.5)$$

In addition, the dispersion coefficient is determined using the Fischer routing method mentioned in the equation 3.6 where the error between the predicted and observed dye concentration in downstream section is minimized by selecting an appropriate value of the dispersion coefficient.

A simple routing procedure given by Fisher et al. (1979) also predicts the distribution of the concentration in the downstream site experiencing the temporal concentration of the upstream site, which can be expressed as

$$C(x_2, t) = \int_{-\infty}^{\infty} \frac{C(x_1,\tau)U}{\sqrt{4\pi D_L(t_2-t_1)}} exp\left[-\frac{[U(t_2-t_1-t+\tau)]^2}{4D_L(t_2-t_1)}\right] d\tau \quad (3.6).$$

Where $C(x_2, t)$ is the predicted value of concentration at station x_2 at time t and $C(x_1, \tau)$ is the observed value of concentration at station x_1 at time τ.

3.10 EXPERIMENTAL PROCEDURE

1) Rhodamine solution of 10000ppb by dilute rhodamine WT with distilled water was prepared and kept it in glass flask.
2) Then started the centrifugal pump and was ensured that overhead tank full so that head of water remains constant.
3) Uniform flow was established in the channel by adjusting the rotatory valve.
4) Then rigid vegetation was kept at distance of 2m from point of injection and was ensured that it is partially submerged.
5) Then pointer gauge was mounted over the fastener and the assembly made on sides of channel and was ensured that water depth remains unchanged.
6) Then at the point of injection that was on starting of channel, a mounted fastener fixed with the help of rod and 40ml burette was fixed in between them and ensured it was just above water surface and add tracer into it.
7) On collection points that was at 1m, after and before vegetation and at 4m, collection bottles with their rack was kept with their lid open
8) Then two sample of pre-concentration of water was taken with the help of Biles.

9) Then burette valve was open as the burette going to empty immediately collection was started and the total time taken by all four persons was noted down and all 200 samples from four locations taken.
10) Then post-concentration of water sample was taken. It was ensured how much concentration of water changed after and before experiment.
11) With the help of pointer gauge the depth of water in between channel and at the v notch was noted down.
12) Then valve was closed and all the instrument kept into laboratory.
13) Then the trilogy fluorometer was switched on and put the green module into the fluorometer and used the stored calibration option which gives concentration unit in ppb.
14) With the help of fluorometer the concentration was measured of all the 200 samples.

CHAPTER 4

EXPERIMENTAL DATA

Experimental data are given in two sections of this chapter. In the first section, the hydraulic data for flows in the experiments are given and in second section the data from the experiments performed to observe the longitudinal dispersion are given.

4.1 Hydraulic Data

Twenty-seven different discharge are used in this experiment with nine different configurations of rigid vegetation. The hydraulic data for each flow is given in Table 4.1.

Table 4.1 Summary of hydraulic data

Depth at V-notch (m)	Depth at channel (m)	"q" (m3/s)	"v" (cm/s)	"Re"	"Fr"	"u*"	Relative density
0.065	0.102	0.002	2.578	3267.963	0.026	0.027	0.09
0.079	0.113	0.003	3.806	5335.040	0.036	0.032	0.09
0.049	0.081	0.001	1.566	1581.784	0.018	0.022	0.09
0.085	0.125	0.004	4.091	6366.079	0.037	0.032	0.16
0.071	0.103	0.002	3.151	4045.203	0.031	0.030	0.16
0.051	0.084	0.001	1.690	1766.522	0.019	0.023	0.16
0.085	0.122	0.004	4.137	6272.873	0.038	0.033	0.26
0.051	0.086	0.001	1.655	1766.522	0.018	0.022	0.26
0.063	0.102	0.002	2.358	2998.826	0.024	0.026	0.26
0.103	0.126	0.006	6.555	10265.099	0.059	0.041	0.33
0.057	0.083	0.001	2.295	2354.588	0.026	0.027	0.33
0.071	0.109	0.002	2.998	4045.203	0.029	0.029	0.33
0.063	0.126	0.002	1.932	3022.721	0.017	0.022	1.00
0.045	0.084	0.001	1.234	1291.043	0.014	0.020	1.00
0.083	0.117	0.003	4.127	5980.135	0.039	0.033	1.00
0.102	0.130	0.006	6.166	9992.960	0.055	0.039	0.52
0.107	0.128	0.006	7.093	11291.950	0.063	0.042	0.52
0.068	0.108	0.002	2.705	3630.773	0.026	0.027	0.52
0.063	0.102	0.002	2.364	2998.826	0.024	0.026	0.19
0.090	0.122	0.004	4.849	7384.839	0.044	0.035	0.19
0.111	0.135	0.007	7.372	12406.010	0.064	0.042	0.19
0.074	0.106	0.002	3.359	4426.322	0.033	0.030	0.36
0.117	0.144	0.008	7.879	14151.072	0.066	0.043	0.36
0.058	0.082	0.001	2.411	2459.037	0.027	0.027	0.36

Depth at V-notch (m)	Depth at channel (m)	"q" (m3/s)	"v" (cm/s)	"Re"	"Fr"	"u*"	Relative density
0.108	0.132	0.007	7.050	11557.883	0.062	0.042	0.64
0.070	0.104	0.002	3.027	3904.070	0.030	0.029	0.64
0.120	0.150	0.008	8.069	15044.323	0.067	0.043	0.64

4.1.1 Water Depth. The water depth here was in between 0.07 to 0.15 m at the channel and as shown in table 4.1. The depth measured in channel was the distance between the water surface and the bottom of the channel. The depth at the crest is the total depth measured just above the crest (v-notch) formation and it is in between the surface of channel and the water surface over crest. The average depth at crest is around 10cm.

4.1.2 Discharge and Velocity. The discharge measured is the total water entering from the upstream end of channel. It is measured with the help of V-notch outlet using equation 4.1 given below.

$$Q = \frac{8}{15} \times C_d \times \sqrt{2g} \times tan\frac{\theta}{2} \times H^{\frac{5}{2}} \quad (4.1)$$

Where,

C_d = coefficient of discharge (0.72)

g = acc. due to gravity (9.81 m/s^2)

Θ = angle of v- notch 90°

H = Depth measured at v-notch

Q = discharge in channel (m^3/s)

Discharge is given in column 3 in table 4.1. The velocity of water in channel was measured by dividing the discharge with the area of channel (i.e. 0.7m width of channel and depth of water at particular discharge value). Velocity is given in column 4 table 4.1.

4.1.3 Reynold number and Froude Number. Reynold number and Froude number are given in column 5 and 6 in table 4.1 and were calculated using depth of water and velocity given in column 2 and 4 of table 4.1. A kinematic viscosity of 0.804×10^{-6} m^2/s, at 30°c, was used in the calculation. The Reynold number is given by Equation 4.2.

$$R_e = \frac{VD}{\rho} \quad (4.2)$$

Where,

Re = Reynold number,

V = Velocity of water in m/s,

D = depth of water in channel,

ρ = Kinematic viscosity of water at 30^oc ($m^{2/}$s).

The Froude number was calculated using equation 4.3 given below

$$F_r = \frac{V}{\sqrt{gD}} \quad (4.3)$$

Where,

Fr = Froude number,

V = average velocity of water in channel,

g = acc. due to gravity,

D = hydraulic mean depth in 'm'

4.1.4 Shear velocity. The bottom shear velocity, $U^{*,}$ given in column 7 of table 4.1 was calculated using equation 4.4 given below.

$$U^* = \sqrt{gDS} \quad (4.4)$$

Which is valid for infinite wide channels but it gives us slightly more value when used for channel having finite width and it is due to shear of walls of channel.

4.2 Experiments with fluid tracer.

4.2.1 Introduction. In this section, data are presented from the experiments performed to calculate the Longitudinal Dispersion with different configurations of rigid vegetations. Although all the data and results are given in chapter 5, this section is just including the tables of data used for subsequent analysis.

Because of large volume of data and tables, the concentrations of tracer observed at all points of for all experiments were not included in this chapter. Instead, these data are given in appendix.

4.2.2 Dispersion coefficient using method of moment and Fischer Routing method.

In this experiment dispersion coefficient was calculated using two methods: method of moment and Fischer routing method. After measuring the concentration using fluorometer the dispersion coefficient was estimated using a program made in fortran.

In fortran program, while calculating dispersion coefficient using moment method, the input in notepad file consisting of time duration for taking one sample and number of sample taken was added. The output file consisted of cloud velocity, tcu, tcd, σcu^2, σcd^2 and D_L which are given in column V to X in table 4.2.

For Fischer routing method the value of tcd, tcu, ntu, u, incr, dlmax, dlmin and h are given as in input file in notepad and output file is consisted of RMS, D_L and concentration value as given in table 4.2 of column XI and XII. The least RMS value is taken for comparison.

Where,

tc = time of travel of dye centroid and subscript u and d means upstream and downstream station, respectively.

σc = variance of the time-concentration curve, and subscript ‘u’ and ‘d’ means upstream and downstream station, respectively.

ntu = number of concentration value taken,

U = cloud velocity,

And h = time duration for taking one sample.

Table 4.2 Estimation of dispersion coefficient using method of moment and Fisher routing method

Sr. No.	Mean Velocity (cm/sec)	Reynolds Number	Froude Number	Cloud Velocity (m/sec)	tcu (sec)	tcd (sec)	σcu²	σcd²	DL(m^2/s) (Method of Moment)	DL(m^2/s) (Fischer Routing)	RMS (error)
I	II	III	IV	V	VI	VII	VIII	IX	X	XI	XII
WITH RIGID VEGETATION OF φ12MM, C-C DISTANCE 50MM IN STAGGERED IN 12 ROWS PRE-COLLECTION FROM PI AT 1M AND 2M											
1	3.35890	4426.322	0.0330	0.107645	34.34428	52.92388	46.4581	50.44795	0.001244	0.0005	22.51731
2	7.8791	14151.0	0.0662	0.05072	35.75392	75.18577	51.64205	54.26026	0.00085	0.0001	14.485
3	2.41105	2459.03	0.0269	0.047608	33.36446	75.37361	53.33392	56.09049	0.00074	0.00005	16.654
		INTERMEDIATE COLLECTION POINT BEFORE AND AFTER VEGETATION									
1	3.35890	4426.32	0.0330	0.02814	52.92388	123.9934	46.4581	68.72042	0.000124	0.00005	40.42653
2	7.8791	14151.0	0.0662	0.04078	75.18577	124.218	54.26026	64.58785	0.000175	0.00005	27.72
3	2.41105	2459.036	0.0269	0.04114	75.37361	123.9766	56.09049	67.7051	0.00020	0.0001	13.254
POST CI AFTER VEGETATION AT DISTANCE 3M AND 4M											
1	3.35898	4426.322	0.033	0.046202	123.993	167.280	68.7204	230.966	0.0040	0.001	30.758
2	7.879128	14151.07	0.0662	0.06612394	124.218	154.4642	64.58785	149.5189	0.006138	0.002	12.85
3	2.411055	2459.0367	0.0269	0.07150358	123.9766	151.9473	51.21737	67.7051	0.001506	0.00005	11.4391

CHAPTER 5

RESULTS AND DISCUSSIONS

Series of experiments were carried out to determine the longitudinal dispersion Coefficient for a flow range corresponding to the range of Reynolds numbers 1000 <Re <16000. The tests were carried out using a recirculation system where the channel length is 6m, and internal width of 0.7m. The flow rate was obtained by measuring the discharge through v-notch.

Rhodamine WT dye injections were performed using a burette at the starting point called point of injection just after the channel start. For each injection, Rhodamine WT at a concentration ranging from 10000-15000 ppb were injected for a period of time. The response of the dye to the flux was recorded as an average cross-sectional concentration depending on the time profiles using Turner Designs fluorometers. The instruments were calibrated before start of the test. The injections were made at a distance of 50cm downstream from the beginning of the test section, giving sufficient length to allow the flow to become fully developed (White 2008). The rhodamine concentration present in the samples collected from four points were measured using fluorometer. The cloud velocity, centroid of the concentration-time curve and temporal variance of a tracer wave is obtained for each site given by equation 5.1.

$$U_C = \frac{x_2 - x_1}{t_2 - t_1} \tag{5.1}$$

Where,

U_C = velocity of tracer cloud,

t_1 and t_2 are the time of travel of the centroid of the concentration-time curve at u/s and d/s.

And

$$\sigma^2 = \int \frac{C(t)t^2 dt}{\int C(t) dt} - t_c^2 \tag{5.2}$$

Where,

σ^2 = variance of the concentration,

t_c = time of travel the concentration-time curve.

It is found that the interval between time and the centre and the temporal variance of a tracer wave increases at the downstream level and thus eliminates the inconsistency. The mean velocity and velocity of the cloud are also compared for different flow conditions and the cloud velocity is found to be greater than the mean velocity in all cases as shown in the table 5.1. The inert chemical contaminant moves from one point to another in water due to the regulation of two processes dominated by water velocity and dispersion. Since both processes are responsible for water transport, it is expected that the cloud will take less time to reach the sampling station. Therefore, it was expected that the velocity of the cloud would be greater than the mean velocity which was also confirmed in the present experiment.

The maximum and minimum percentage of the difference between the average velocity and the velocity of the cloud is approximately 80% and 20% respectively for the velocity less than 0.0250 m/s and 50% and 10% respectively for a velocity greater than 0.70 m/s. This shows that the percentage difference between the mean velocity and the cloud velocity is higher for the lower Reynolds number and this percentage decreases for higher Reynolds number. When the Reynolds number increases, the transport of inert chemical contaminants is more dominated by the velocity of the water compared to the dispersion process. Thus, there is less time difference to reach the sampling station between the cloud and the water particle for a greater number of Reynolds.

As a result, the percentage difference between the mean velocity and the cloud velocity is greater for the lower Reynolds number and this percentage decreases for the higher Reynolds number. The speed at which the cloud propagates, the decrease in the maximum concentration and the resulting concentration profile along the stream are of great importance in pollution control.

Table 5.1 Mean velocity and cloud velocity are compared for different flow conditions

Sr. No.	**Velocity (m/s)**	**Depth (m)**	**R**	**u***	**Cloud Velocity**
1	0.0258	0.102	0.0789	0.04703	0.0751
2	0.0381	0.113	0.0852	0.04888	0.0876
3	0.0157	0.081	0.0659	0.04298	0.0542
4	0.0409	0.125	0.0922	0.05082	0.0462

Sr. No.	Velocity (m/s)	Depth (m)	R	u*	Cloud Velocity
5	0.0315	0.103	0.0797	0.04726	0.0448
6	0.0169	0.084	0.0678	0.04358	0.0448
7	0.0414	0.122	0.0904	0.05034	0.0643
8	0.0166	0.086	0.0689	0.04395	0.0985
9	0.0236	0.102	0.0791	0.04710	0.0663
10	0.0656	0.126	0.0926	0.05094	0.0925
11	0.0229	0.083	0.0668	0.04326	0.0978
12	0.0300	0.109	0.0828	0.04818	0.0802
13	0.0193	0.126	0.0925	0.05093	0.0645
14	0.0123	0.084	0.0678	0.04360	0.0813
15	0.0413	0.117	0.0874	0.04950	0.0568
16	0.0617	0.130	0.0950	0.05159	0.0585
17	0.0709	0.128	0.0937	0.05125	0.0782
18	0.0271	0.108	0.0825	0.04808	0.0483
19	0.0236	0.102	0.0790	0.04705	0.0585
20	0.0485	0.122	0.0907	0.05042	0.0601
21	0.0737	0.135	0.0976	0.05230	0.0204
22	0.0336	0.106	0.0813	0.04774	0.1048
23	0.0788	0.144	0.1022	0.05353	0.0510
24	0.0241	0.082	0.0664	0.04315	0.0480
25	0.0705	0.132	0.0957	0.05180	0.0721
26	0.0303	0.104	0.0800	0.04735	0.0659
27	0.0807	0.150	0.1050	0.05424	0.1102

The variation of the rhodamine concentration over time for different cases is also an analysis and as shown in the from figure 5.1 to figure 5.3. It shows the variation of rhodamine concentration over time for different Reynolds numbers at a distance of 2 m downstream from the point of injection in the presence of different rigid vegetation configurations.

It is found that as the time increases as the concentration increases to its peak and then it decreases. The variation of Reynolds number considered is covering transition and turbulent flow. The tracer is propagated in all directions by the effects molecular and turbulent diffusion. However, both broadcasts mechanisms are important with respect to longitudinal dispersion due to their ability to diffuse the tracer radially. As radial diffusion increases, each particle of the tracer has a greater number of radial positions and corresponding speeds. This reduces the effects of differential advection. Therefore, there is an inverse relationship between molecular diffusion and longitudinal dispersion.

It is also found that the time taken to reach the peak concentration is affected by the presence of rigid vegetation as well as due to Reynolds number in transition and in turbulent zone may be due to decrease in lateral movement of the cloud. But the magnitude of the peak concentration increases for further increase in the Reynolds number due to the cloud reaching the test section earlier than the start of sufficient lateral movement. It is found that the peak concentration is maximum for slow moving cloud due to simultaneous movement of the cloud at small velocity of flow.

Figures 5.1, shows the variation of rhodamine WT concentration with time for different Reynolds number at 4m downstream from the point of injection in the absence as well as in the presence of rigid vegetation. The concentration time curve shown in figures 5.1 for the case of without vegetation having different Reynolds numbers are compared with the different Reynolds number of rigid vegetation of diameter 12, 16 and 20mm placed in 6, 9 and 12 rows in staggered manner and also compared with various Reynolds number after the vegetation (4m from point of injection). The peak concentration for all configurations is compared with the peak concentrations for the case of without vegetation.

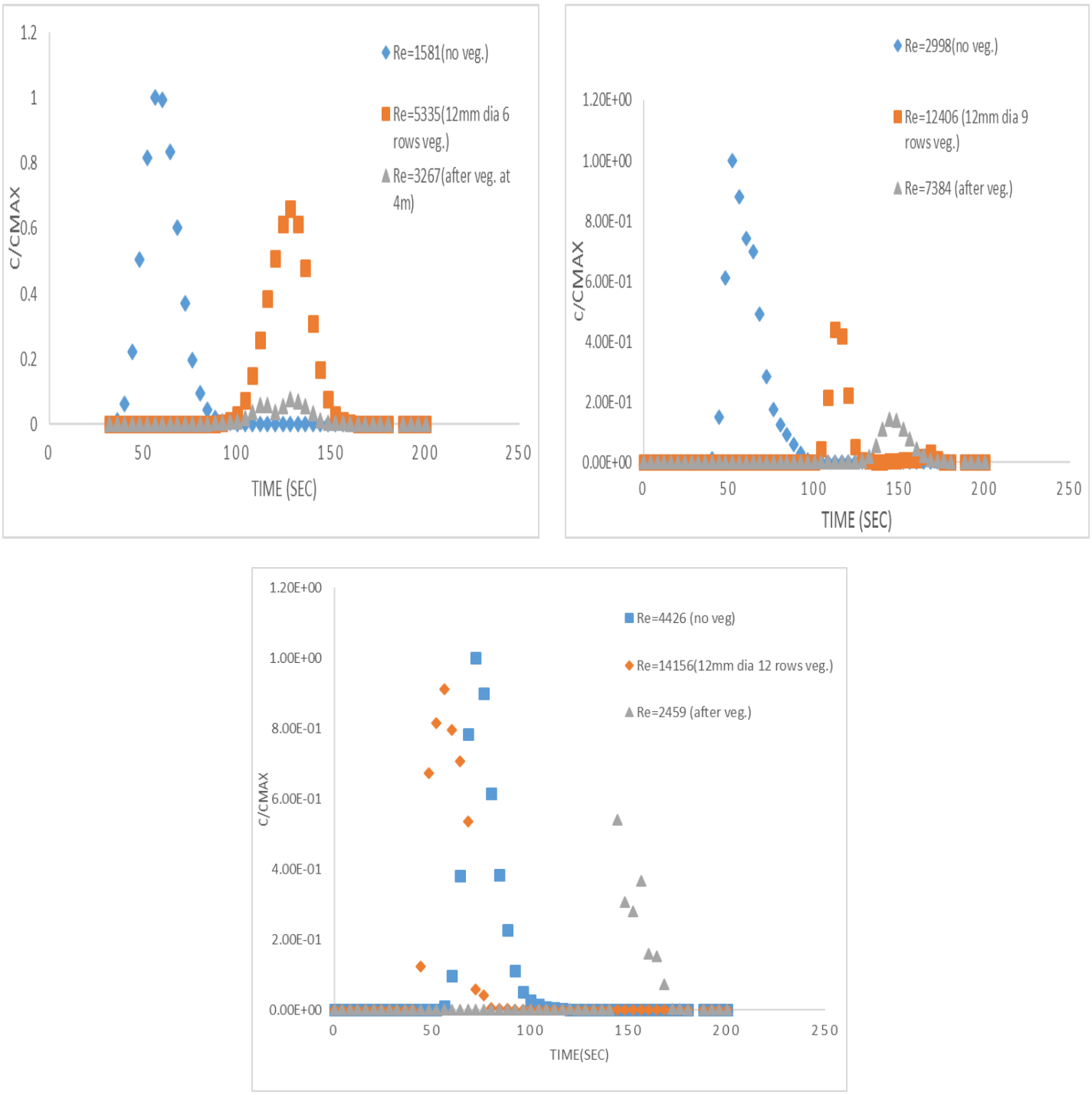

Figure 5.1 Variation of concentration with time for different Reynolds number in presence of 12mm diameter rigid vegetation in 6,9 and 12 rows

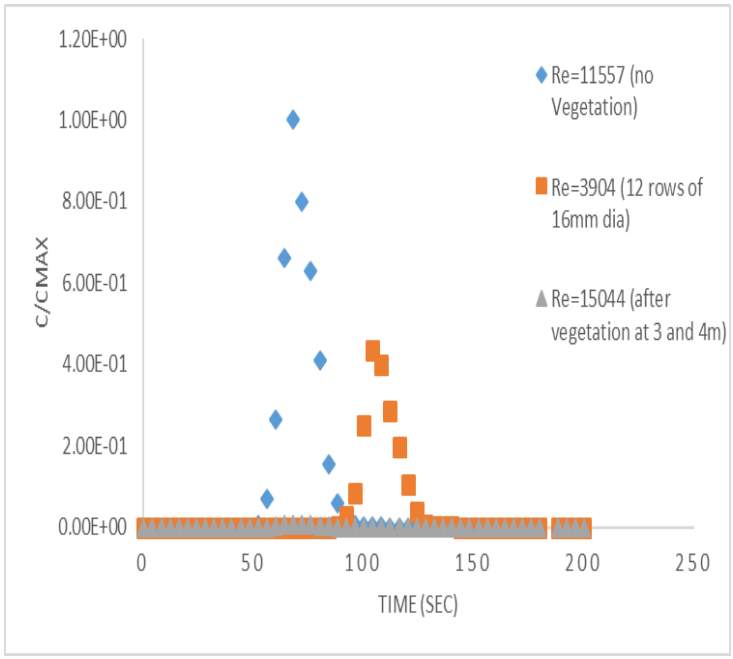

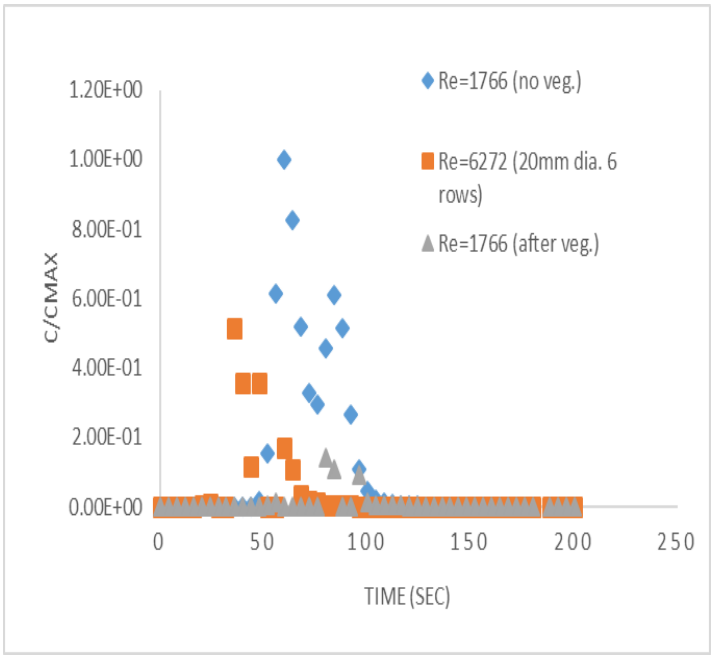

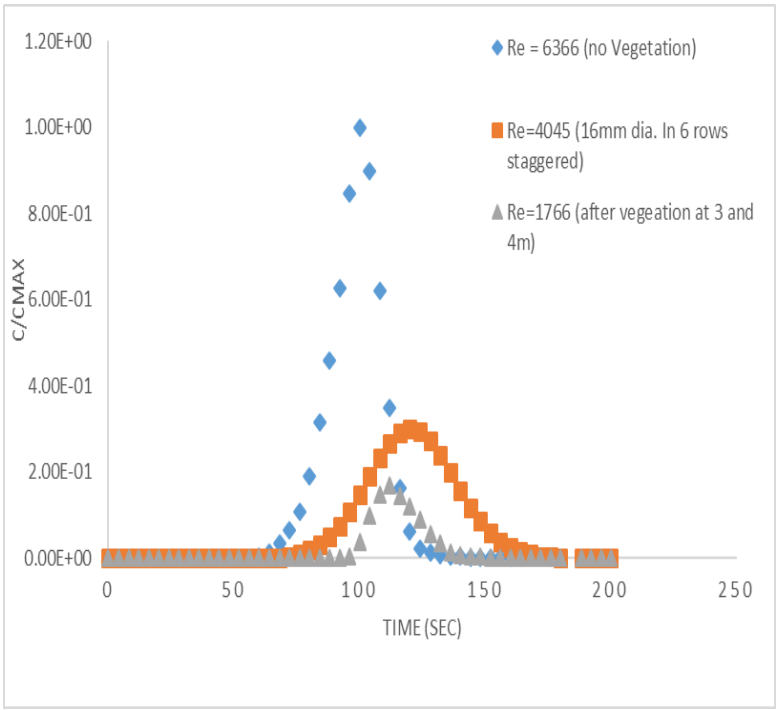

Figure 5.2 Variation of concentration with time for different Reynolds number in presence of 16mm diameter rigid vegetation in 6,9 and 12 rows

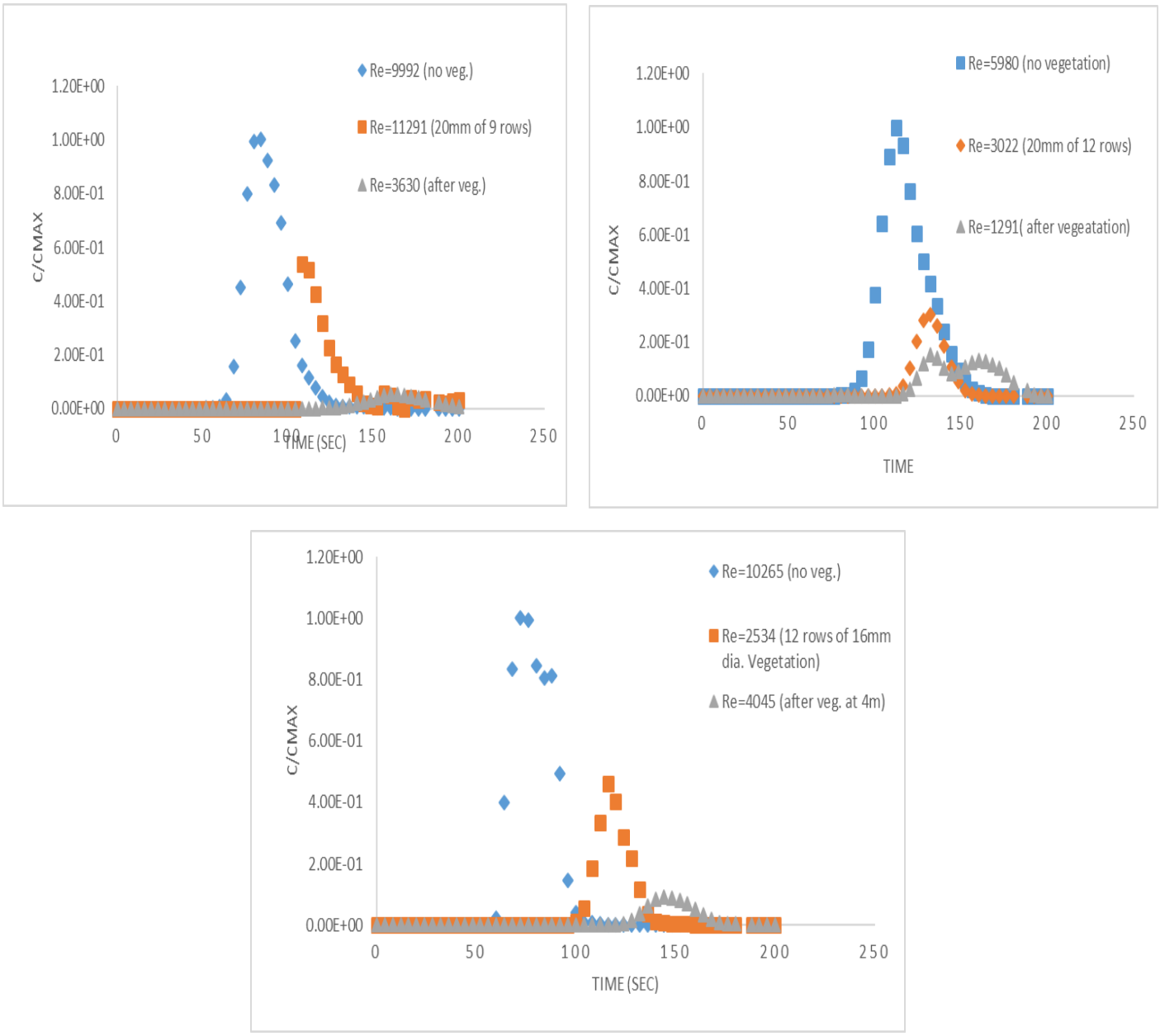

Figure 5.3 Variation of concentration with time for different Reynolds number in presence of 20mm diameter rigid vegetation in 6,9 and 12 rows

Table 5.2 Percentage of reduction of peak concentration in the presence of rigid vegetation of different configuration

Configuration	**12mm dia. 6 rows**	**12mm dia. 9 rows**	**12mm dia. 12 rows**
Percentage reduction of peak concentration	34 (for Re = 5335)	57 (for Re = 12406)	8 (for Re =14156)
Percentage reduction of peak concentration at 4m from PI	92 (for Re =3267)	85 (for Re =7384)	46 (for Re =2459)
Configuration	**16mm dia. 6 rows**	**16mm dia. 9 rows**	**16mm dia. 12 rows**
Percentage reduction of peak concentration	70 (for Re =4045)	54 (for Re = 2534)	57 (for Re = 3904)
Percentage reduction of peak concentration at 4m from PI	83.1 (for Re =1766)	90.83 (for Re =4045)	100 (for Re = 15044)
Configuration	**20mm dia. 6 rows**	**20mm dia. 9 rows**	**20mm dia. 12 rows**
Percentage reduction of peak concentration	48.7 (for Re =6272)	48.4 (for Re = 11291)	69.8 (for Re= 3022)
Percentage reduction of peak concentration at 4m from PI	85.7 (for Re =1766)	94.79 (for Re =3630)	84.7 (for Re = 1291)

The table 5.2 shows that the percentage reduction of the maximum concentration at a point decreases significantly in the presence of rigid vegetation. It is found that the maximum concentration is higher in the presence of 16 mm of diameter compared to the rigid vegetation of 12 and 20 mm in diameter. The percentage reduction in the maximum concentration is

approximately 34%, 57% and 8% for the case of a diameter of 12 mm placed respectively in 6, 9 and 12 rows. The percentage reduction in the maximum concentration is less than 12 mm diameter of the rigid vegetation placed in 12 rows due to the high Reynolds number of 14156 compared to the Reynolds number of 4426 for the unfertilized case. Similarly, the percentage reduction in maximum concentration is about 70%, 54% and 57% for the case of 16 mm diameter and the percentage reduction in the maximum concentration is about 48.7%, 48.4% and 69.8% for the case of 20 mm Diameter of the rigid vegetation placed respectively in 6, 9 and 12 rows. And at a distance of 4m from the injection site with a vegetation at 2m of dimensions 600x800mm, the concentration is about 92%, 85% and 46% in the case of 12 mm diameter, 83.1, 90.83 and 100% in the case of 16mm diameter and 85.7%, 94.79% and 84.7% in the case of 20 mm diameter.

Decreasing the maximum concentration in higher diameter vegetation can be attributed to increased adsorption of contaminants due to an increase in surface area. In addition, a large tail end with multiple peaks is found in the concentration-time curve as shown in the above graphs for the case of flow through vegetation due to adsorption and desorption of rhodamine to the surface of the vegetation. The peaks in the tail end have a lower concentration than the peak of the rising curve.

The dispersion coefficient is determined by method of moment using the equation

$$\sigma_t = \frac{1}{2}\frac{d\sigma_x^2}{dt} \tag{5.3},$$

Where,

σ_x^2 is the variance of spatial variance of longitudinal direction,

$$D_L = \left(\frac{U_C^2}{2}\left(\frac{\sigma_t^2(x_2)-\sigma_t^2(x_1)}{t_2-t_1}\right)\right. \tag{5.4},$$

Where,

U_C is the velocity of tracer cloud, σ_t^2 is the variance of the concentration-time curve, $t_2\ and\ t_1$ is the time of travel of the centroid of the concentration-time curve at upstream and downstream site respectively.

The diffusion process is dominated by mechanical diffusion (Nepf, 1999, Serra et al. 2004). Nepf (1999) Suggested that channel eddies (i.e. depth of flow) may persist in between vegetation. When the diameter of the vegetation is much smaller than the depth of flow (d << h).

The velocity of tracer cloud can be expressed as

$$U_C = \frac{x_2 - x_1}{t_2 - t_1} \quad (5.4),$$

Where,

U_C is the velocity of tracer cloud, and t_1 and t_2 are the time of travel of the centroid of the concentration-time curve at u/s and d/s.

The centroid of the concentration-time curve and temporal variance of a tracer wave (Day, 1975)

at a particular site can be expressed as

$$t_c = \frac{\int C(t)tdt}{\int C(t)dt} \quad (5.5),$$

$$\sigma^2 = \int \frac{C(t)t^2dt}{\int C(t)dt} - t_c^2 \quad (5.6)$$

In addition, the dispersion coefficient is determined using the Fischer routing method mentioned in the equation. 6 where the error between the predicted and observed dye concentration in downstream section is minimized by selecting an appropriate value of the dispersion coefficient.

A simple routing procedure given by Fisher et al. (1979) also predicts the distribution of the concentration in the downstream site experiencing the temporal concentration of the upstream site, which can be expressed as

$$C(x_2,t) = \int_{-\infty}^{\infty} \frac{C(x_1,\tau)U}{\sqrt{4\pi D_L(t_2-t_1)}} exp\left[-\frac{[U(t_2-t_1-t+\tau)]^2}{4D_L(t_2-t_1)}\right] d\tau \quad (5.7).$$

Where,

$C(x_2,t)$ is the predicted value of concentration at station x_2 at time t and $C(x_1,\tau)$ is the observed value of concentration at station x_1 at time τ.

We predict from analysis that the dispersion coefficient value of the channel determination using the current method and the dispersion coefficient value using the Fischer routing method for no vegetation and in presence of vegetation. It is found that the value obtained by time method is different from the value obtained by the Fischer routing method, but the trend is almost similar. The non-vegetation longitudinal dispersion coefficient is between 0.0001 and 0.005 for the Reynolds number from 1766 to 11557. Although all the value of the longitudinal dispersal coefficient having vegetation in the channel has a magnitude greater than that of the dispersion coefficient Longitudinal axis without vegetation in the channel, it is found that the value of the dispersion coefficient is 0.01 and 0.05 because the experiment was carried out at a very high Reynolds number. Therefore, it can be concluded that the presence of vegetation affects the dispersal coefficient.

From Table 5.3 in column XI, the longitudinal dispersion coefficient for 6 rows of rigid vegetation 12 mm in diameter is 0.0005 for Reynolds number 3267, for 9 rows of rigid vegetation 12 mm in diameter is 0.0001 for Reynolds number 7384 and for 12 rows it is 0.0005 for Reynolds number 4426. And as the diameter increases from 12 mm to 16 mm, the longitudinal dispersion coefficient for 6 rows of rigid vegetation of 16 mm diameter is 0.005 for Reynolds number 6366, for 9 lines of diameter 16 mm it is 0.0001 for Reynolds number 10265 and 12 rows of 16 mm diameter It is 0.0001 for Reynolds number 11557 and again for the diameter 20 mm, the longitudinal dispersion coefficient for 6 rows of 20 mm diameter of rigid vegetation is 0.025 for Reynolds number 6272, for 9 lines of 20 mm diameter it is 0.002 for Reynolds number 3630 and 12 lines of 20 mm in diameter, it is 0.004 for Reynolds number 3032.

Table 5.3 Estimation of dispersion coefficient using moment and Fischer routing method

Sr. No.	Mean Velocity (cm/sec)	Reynolds Number	Froude Number	Cloud Velocity (m/sec)	tcu (sec)	tcd (sec)	σcu²	σcd²	DL(m^2/s) (Method of Moment)	DL(m^2/s) (Fischer Routing)	RMS (error)
I	II	III	IV	V	VI	VII	VIII	IX	X	XI	XII
WITHOUT ANY RIGID VEGETATION											
1	3.359	4426.322	0.033	0.108	34.344	52.924	46.458	50.448	0.001	0.001	22.517
2	4.1270	5980.13	0.0386	0.056821	34.70959	69.90768	67.847	143.03	0.00344	0.001	4.166
3	2.411	2459.037	0.027	0.048	33.364	75.374	53.334	56.090	0.00007	0.0005	16.654
WITH RIGID VEGETATION OF φ12MM, C-C DISTANCE 5CM IN STAGGERED IN 12 ROWS											
1	3.35890	4426.322	0.0330	0.107645	34.34428	52.92388	46.4581	50.44795	0.001244	0.0005	22.51731
2	7.8791	14151.0	0.0662	0.04078	75.18577	124.218	54.26026	64.58785	0.000175	0.00005	27.72
3	2.411055	2459.0367	0.0269	0.07150358	123.9766	151.9473	51.21737	67.7051	0.001506	0.00005	11.4391
		WITH RIGID VEGETATION OF 16MM DIA IN 12 ROWS									
1	7.05048	11557.8	0.0620	0.054910	70.75501	107.1782	54.9844	98.45515	0.00179	0.0001	11.5205
2	3.02687	3904.07	0.0300	0.043297	61.60238	107.7939	47.71955	141.2563	0.00189	0.0001	9.630645
3	8.06913	15044.3	0.0666	0.062143	58.04755	90.23088	39.74089	91.08409	3.08E-03	0.00015	18.5253
WITH RIGID VEGETATION OF 20MM DIA IN 12 ROWS											
1	1.93185	3022.72	0.0174	0.070950	59.18857	87.3772	110.6105	210.6439	0.00893	0.004	18.376
2	1.23424	1291.04	0.0136	0.0956	59.85	80.54	114.251	180.352	0.00325	0.0015	10.263
3	4.127063	5980.135	0.0386	0.0359	112.52	139.85	168.22	196.35	0.002946	0.001	7.256
WITH RIGID VEGETATION OF φ12MM, C-C DISTANCE 7.5CM IN STAGGERED IN 9 ROWS											
1	2.36378	2998.826	0.023642	0.052099	48.09954	86.48742	46.21151	109.4352	0.00223	0.0005	9.5892
2	4.848844	7384.839	0.044263	0.052994	59.99259	97.73245	48.44104	57.63076	0.000341	0.0001	10.2565

Sr. No.	Mean Velocity (cm/sec)	Reynolds Number	Froude Number	Cloud Velocity (m/sec)	tcu (sec)	tcd (sec)	σcu²	σcd²	DL(m^2/s) (Method of Moment)	DL(m^2/s) (Fischer Routing)	RMS (error)
I	II	III	IV	V	VI	VII	VIII	IX	X	XI	XII
3	7.372085	12406.01	0.06402	0.035954	61.83445	117.461	38.93414	164.9716	0.001464	0.0001	7.060527
WITH RIGID VEGETATION OF 16MM DIA IN 9 ROWS											
1	6.555313	10265.09	0.0590	0.0291643	78.5461	147.123	62.27907	101.2575	0.00024	0.0001	9.65821
2	2.29465	2354.588	0.0255	0.049175	78.52924	119.1995	67.14688	86.7728	0.00058	0.00025	6.134708
3	2.997551	4045.202	0.0291	0.050147	83.54277	123.4254	60.13997	91.68018	0.00099	0.0005	22.5452
WITH RIGID VEGETATION OF 20MM DIA IN 9 ROWS											
1	6.16603	9992.95	0.0546	0.035233	64.5866	96.621	76.562	110.5156	0.00353	0.0015	18.622
2	7.09275	11291.95	0.0633	0.058571	53.7031	124.5973	87.84926	175.7213	0.002568	0.001	20.674
3	2.705413	3630.773	0.0263	0.0325	35.266	61.295	45.695	69.6522	0.004556	0.002	19.685
WITH RIGID VEGETATION OF 12MM DIA IN 6 ROWS											
1	0.02578	3267.963	0.025802	0.1052558	56.07766	75.07899	181.8403	220.4318	0.001125	0.0005	17.85469
2	0.03232	5335.03	0.036215	0.047556	45.99471	88.0499	138.2636	256.7097	0.003184	0.001	22.97431
3	0.0154	1581.783	0.017557	0.068511	121.4921	150.6842	129.3179	142.6701	0.00107	0.0005	25.8548
WITH RIGID VEGETATION OF 16MM DIA IN 6 ROWS											
1	4.091388	6366.078	0.0370	0.0605735	66.45792	99.47565	96.71056	238.9364	0.00790	0.005	7.363772
2	3.151495	4045.202	0.0313	0.048208	79.35579	120.8422	108.8552	124.9623	0.00045	0.0002	18.2542
3	1.689808	1766.522	0.0186	0.050624	71.73651	111.2433	64.48181	108.6975	0.001434	0.0005	22.2542
WITH RIGID VEGETATION OF 20MM DIA IN 6 ROWS											
1	1.689808	1766.522	0.0186	0.05983	96.3593	109.683	49.3834	128.653	0.0356	0.015	9.642
2	4.137317	6272.872	0.0379	0.1360182	104.5171	119.221	55.903	139.24	0.0524	0.025	17.615
3	1.655342	1766.52	0.0181	0.05636	36.935	64.65933	109.653	139.6824	0.0425	0.002	35.652

Therefore, it is concluded that the dispersal coefficient is affected in the presence of vegetation and it increases in magnitude when rigid vegetation of different diameters is stored at 2 m from the point of injection. But the coefficient of dispersion decreases with the increase of the rows of rigid vegetation from 6 rows to 9 and 12 rows. When the number of rows of rigid vegetation increases from 6 rows to 9 rows, the longitudinal dispersion coefficient decreases due to the increase in lateral dispersion and the same consequence when vegetation increases from 9 rows to 12 rows.

Thus, the increase in the number of rows of vegetation affects the longitudinal dispersal coefficient and the vegetation diameter also affects the longitudinal dispersion coefficient as the diameter increases. The longitudinal dispersion coefficient increases, but as the number of rows increased, the longitudinal dispersion decreases. So, it is confirmed that the dispersion coefficient is affected in the presence of rigid vegetation and it is inversely related with the density of vegetation till some aspect and then vice versa but it is directly proportional with the diameter of vegetation as the diameter increases the dispersion coefficient is also increases, only in two experiments some irregularities are found there due to higher Reynolds number.

The table 5.3 above shows the magnitude of the longitudinal dispersion coefficient obtained from the Fischer routing method. The figure 5.4-5.6 shows the comparison of the observed and predicted concentration for the case without vegetation as well as with vegetation of 12, 16 and 20 mm diameter present at 6, 9 and in 12 rows. It can be seen that the behaviour of the expected concentration is in agreement with the concentration observed in all cases. It can be seen from the table 5.3 that the dispersion coefficient increases with increasing vegetation diameter. Therefore, it can be concluded that the dispersion coefficient depends on the number of rows of vegetation but depends on the diameter of the vegetation due to the increase in area.

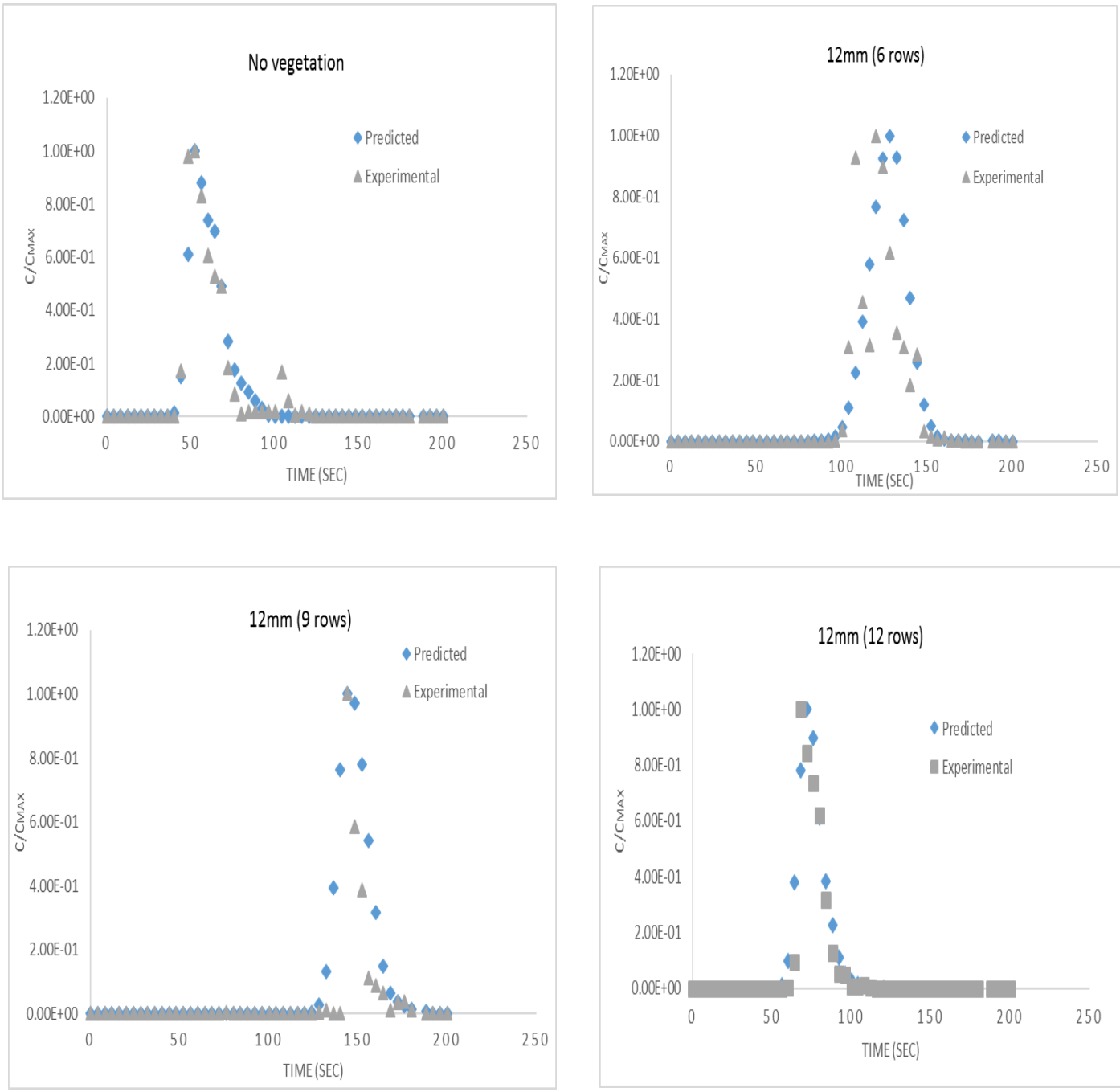

Figure 5.4 Comparison of experimental and predicted concentration for 12 mm diameter rigid vegetation in 6, 9 and 12 rows

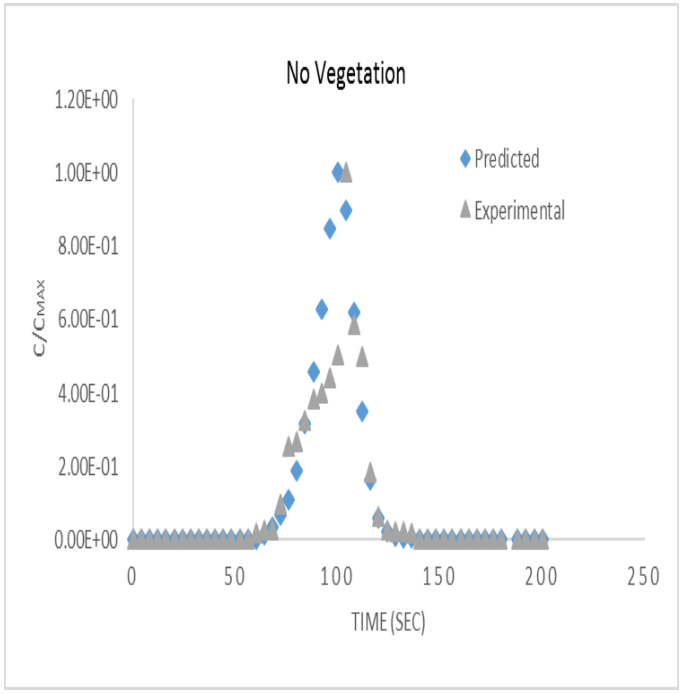

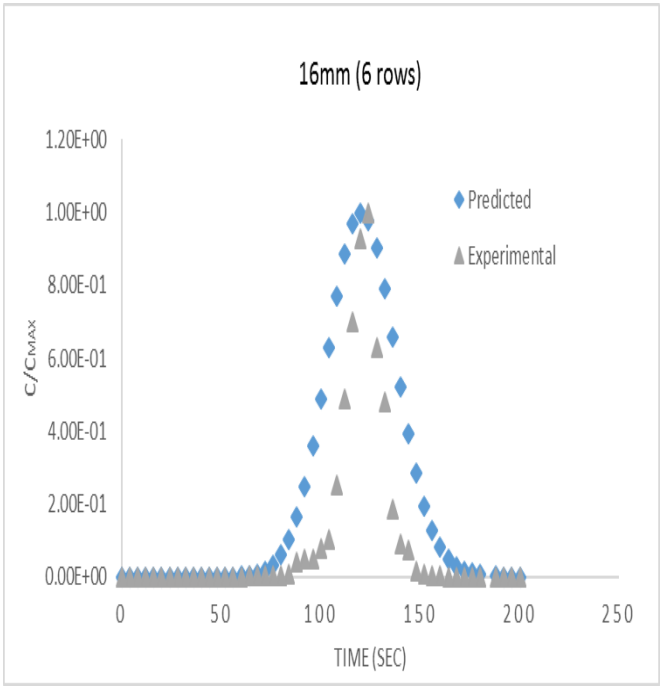

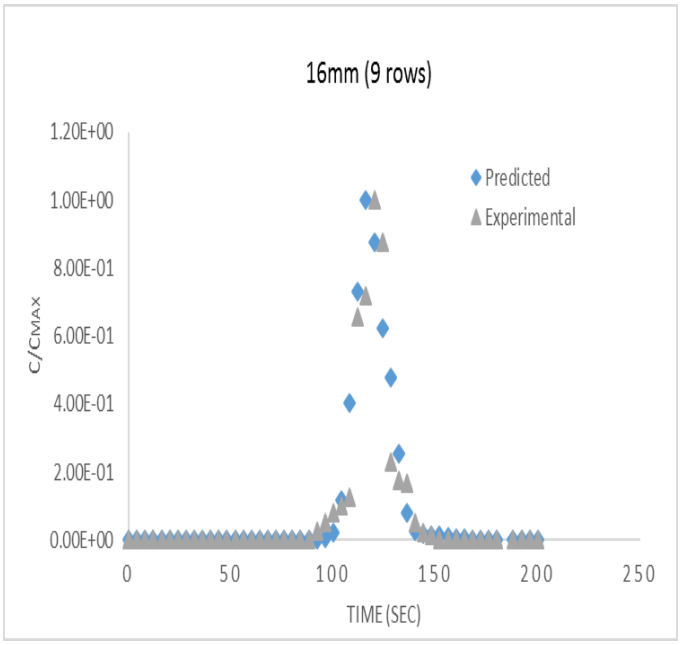

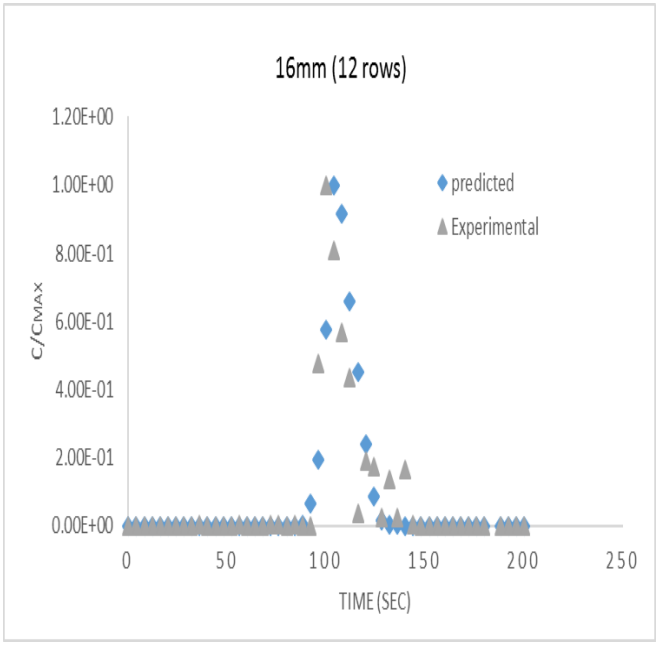

Figure 5.5 Comparison of experimental and predicted concentration for 16mm diameter rigid vegetation in 6, 9 and 12 rows

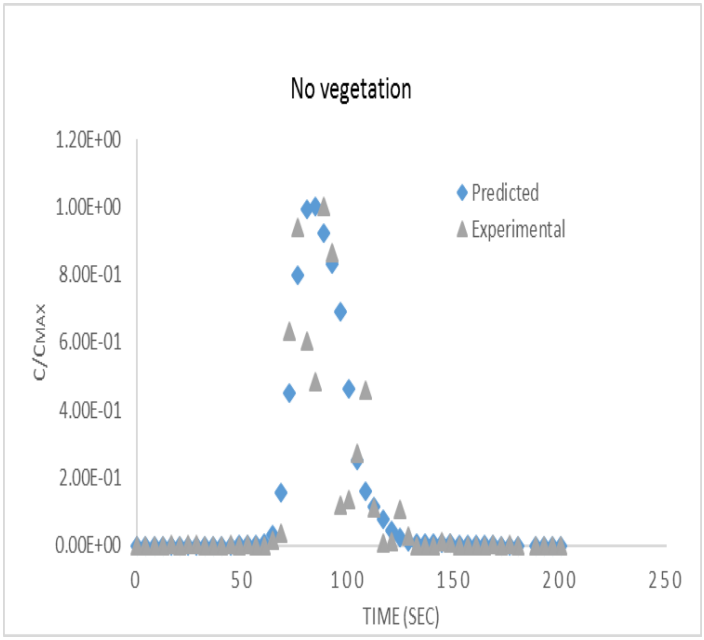

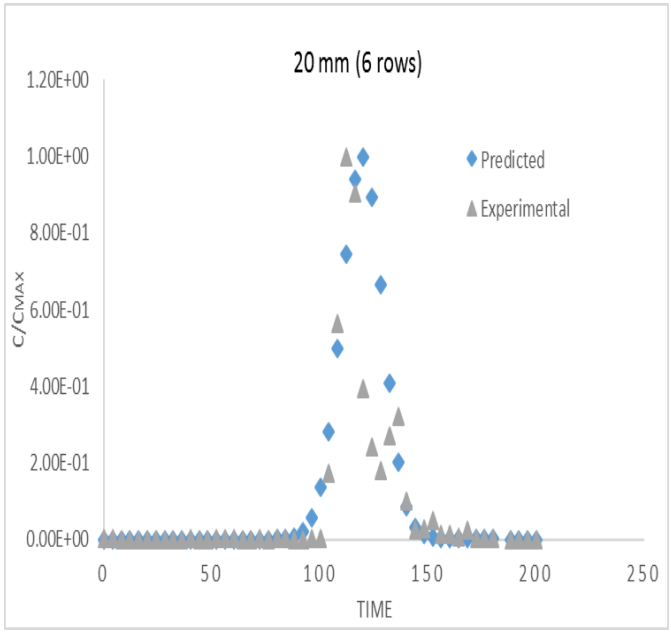

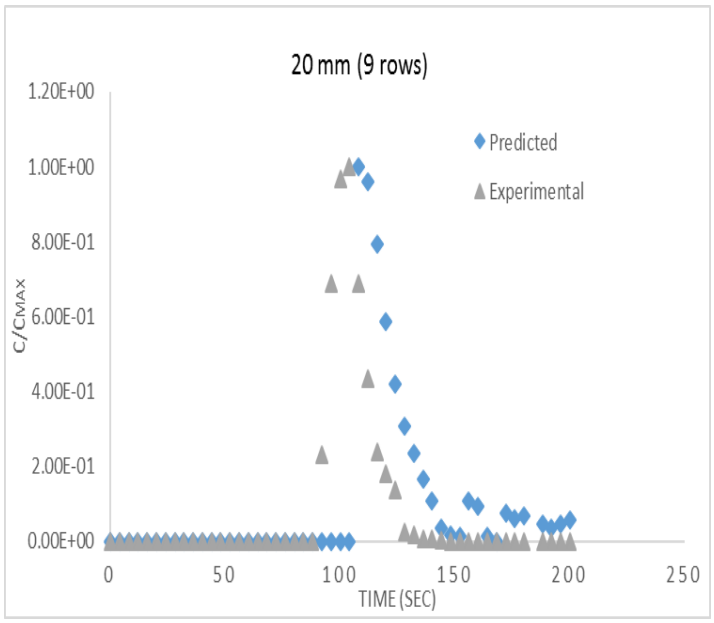

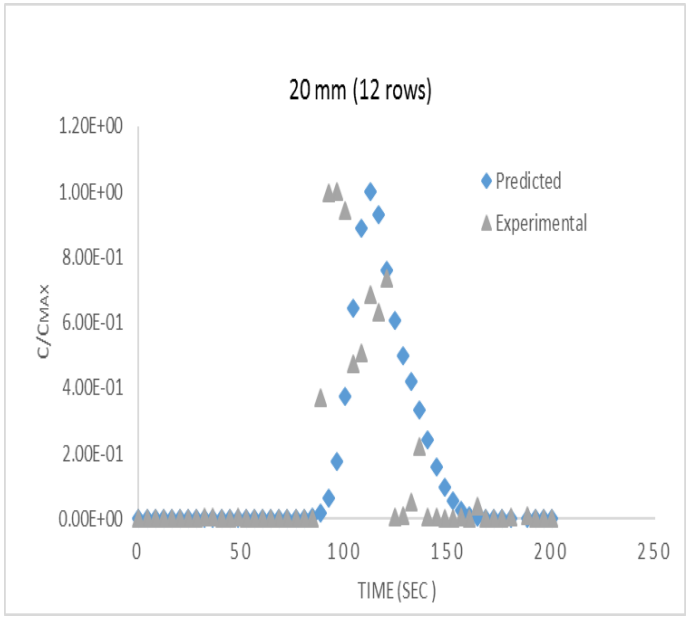

Figure *5.6* Comparison of experimental and predicted concentration for 20mm diameter rigid vegetation in 6, 9 and 12 rows

5.2 Development of equation using SPSS Statistics

IBM SPSS Statistics was used to develop a correlation between D_L and independent parameter such as velocity, depth, density of rigid vegetation and U^*. Data to be used in SPSS was obtained from work done in laboratory of various different configuration and discharge in ours experiment. The new equation of D_L is made using the analysis of longitudinal dispersion of rigid vegetation. The predicted value of D_L by using Elder, Glover, Parker and Fischer equations and were compared with our predicted D_L as shown in table 5.4. The calculated value from Fischer equation are nearly matching with our predicted values. So, by using the parameter such as velocity, depth, density of rigid vegetation made an equation using dimensional analysis.

Table 5.4 Empirical relationship for the estimation of dispersion coefficient

Elder (1959)	$D_L = 5.9 \times H \times U_*$
Glover (1964)	$D_L = 500 \times R \times U_*$
Parker (1961)	$D_L = 14.3 \times R^{1.5} \sqrt{2 \times g \times S}$
Fischer (1975)	$D_L = 0.011 \times \frac{U^2 W^2}{H U_*}$

Where,

R = hydraulic radius,

U_* = shear velocity,

H = depth,

g = acc. Due to gravity,

S = bed slope of the stream,

w = width of stream,

And, Q = flow discharge in the stream.

Table 5.5 Estimation of dispersion coefficient using different empirical relationship

Velocity (m/s)	Depth (m)	R	Relative density	U_*	Elder D_L	Glover D_L	Parker D_L	Fischer D_L	Predicted D_L
0.0258	0.102	0.0789	0.091999992	0.04703	0.02828	1.8560	0.0751	0.00075	0.00500
0.0381	0.113	0.0852	0.091999992	0.04888	0.03250	2.0836	0.0843	0.00142	0.00500
0.0157	0.081	0.0659	0.091999992	0.04298	0.02059	1.4164	0.0573	0.00038	0.00100
0.0409	0.125	0.0922	0.163555559	0.05082	0.03751	2.3420	0.0947	0.00142	0.00050
0.0315	0.103	0.0797	0.163555559	0.04726	0.02878	1.8835	0.0762	0.00110	0.00060
0.0169	0.084	0.0678	0.163555559	0.04358	0.02161	1.4770	0.0597	0.00042	0.00010
0.0414	0.122	0.0904	0.255555551	0.05034	0.03620	2.2756	0.0920	0.00150	0.00100
0.0166	0.086	0.0689	0.255555551	0.04395	0.02225	1.5142	0.0612	0.00039	0.00050
0.0236	0.102	0.0791	0.255555551	0.04710	0.02841	1.8634	0.0754	0.00062	0.00150
0.0656	0.126	0.0926	0.330666657	0.05094	0.03784	2.3585	0.0954	-	-
0.0229	0.083	0.0668	0.330666657	0.04326	0.02106	1.4440	0.0584	0.00080	0.00010
0.0300	0.109	0.0828	0.330666657	0.04818	0.03084	1.9953	0.0807	0.00093	0.00010
0.0193	0.126	0.0925	1	0.05093	0.03780	2.3564	0.0953	-	0.00050
0.0123	0.084	0.0678	1	0.04360	0.02163	1.4780	0.0598	-	0.00250
0.0413	0.117	0.0874	1	0.04950	0.03402	2.1631	0.0875	0.00159	0.00100
0.0617	0.130	0.0950	0.51666667	0.05159	0.03966	2.4492	0.0991	0.00305	0.00100
0.0709	0.128	0.0937	0.51666667	0.05125	0.03871	2.4018	0.0971	0.00413	0.00005

Velocity (m/s)	Depth (m)	R	Relative density	U_*	Elder D_L	Glover D_L	Parker D_L	Fischer D_L	Predicted D_L
0.0236	0.102	0.0790	0.185999999	0.04705	0.02832	1.8581	0.0752	-	0.00100
0.0271	0.108	0.0825	0.51666667	0.04808	0.03061	1.9827	0.0802	-	0.00015
0.0485	0.122	0.0907	0.185999999	0.05042	0.03643	2.2871	0.0925	0.00205	0.00050
0.0737	0.135	0.0976	0.185999999	0.05230	0.04175	2.5515	0.1032	0.00414	0.01000
0.0336	0.106	0.0813	0.359999999	0.04774	0.02985	1.9415	0.0785	-	0.00050
0.0788	0.144	0.1022	0.359999999	0.05353	0.04560	2.7359	0.1107	0.00433	0.00010
0.0241	0.082	0.0664	0.359999999	0.04315	0.02088	1.4334	0.0580	-	-
0.0705	0.132	0.0957	0.639999991	0.05180	0.04028	2.4800	0.1003	0.00392	0.00015
0.0303	0.104	0.0800	0.639999991	0.04735	0.02897	1.8940	0.0766	-	-
0.0807	0.150	0.1050	0.639999991	0.05424	0.04797	2.8461	0.1151	0.00432	0.00300

The shape factor of the bed (Sf), the sinuosity (Sn) are the vertical and transverse irregularities in the natural flow. The present study does not consider these two parameters when the experiment takes place in a straight rectangular channel. Considering four parameters in which three are independent and one is dependent as shown in input file for SPSS below.

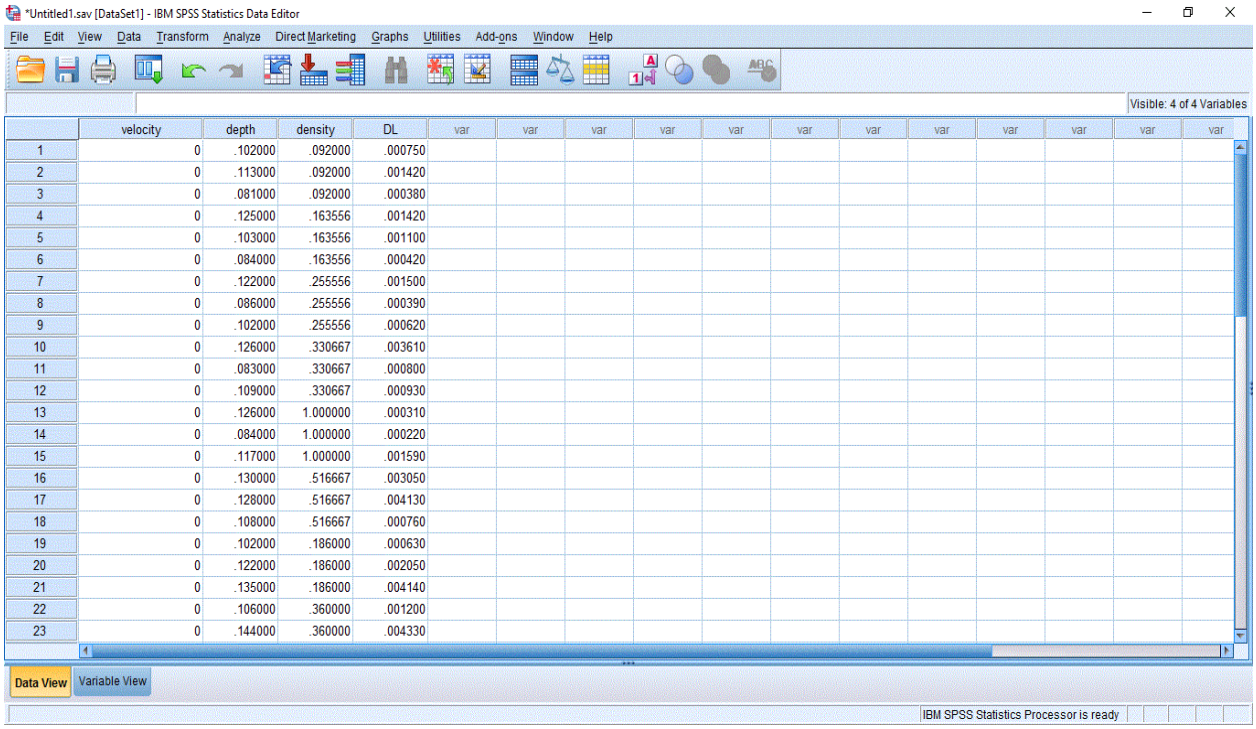

Figure 5.7 Input data editor in IBM SPSS Statistics

Therefore, to establish the relationship, 27 experiments were carried out as shown in table 5.5 above. In output, we get the results in tabular form as shown below.

Table 5.6 Model summary of SPSS contains value of R^2

Model	R	R Square	Adjusted R Square	Std. Error of the Estimate	Change Statistics				
					R Square Change	F Change	df1	df2	Sig. F Change
1	.996[a]	.991	.990	.00014	.991	888.586	3	23	.000

a. Predictors: (Constant), density, velocity, depth

b. Dependent Variable: DL

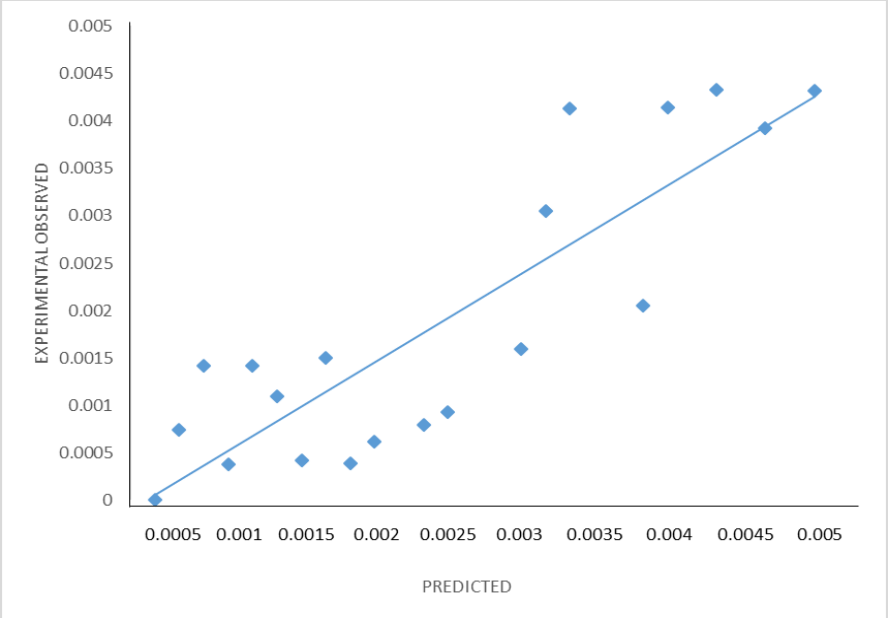

Figure 5.8 Comparison of experimental and estimate dispersion coefficient

It is found that the correlation coefficient R^2 of the established relationship is 0.991 indicating a good correlation between the predicted and observed dispersion coefficient. The table 5.7 shown below represent the value of coefficients of velocity, depth and density and it is found that significance level P-value of the test t for the parameters is less than 0.05 in all three parameters. Therefore, there is a good correlation between the observed and predicted dispersion coefficient.

Table 5.7 Coefficients table of velocity, depth and density

Coefficients

Model		Unstandardized Coefficients		Standardized Coefficients	T	Sig.	Correlations			Collinearity Statistics	
		B	Std. Error	Beta			Zero-order	Partial	Part	Tolerance	VIF
1	(Constant)	.00034265	.000241		1.424	.168					
	velocity	.0789174	.002763	1.190	28.565	.000	.990	.986	.551	.214	4.664
	depth	-.0165625	.003052	-.230	-5.428	.000	.824	-.749	-.105	.207	4.836
	density	.0002207	.000105	.043	2.103	.047	.076	.402	.041	.908	1.101

a. Dependent Variable: DL

$$D_L = 0.00034 + 0.0789v - 0.0166H + 0.0002\rho \quad (5.8)$$

Where v is the flow velocity, H is the flow depth and ρ is the relative density of the rigid vegetation. Therefore, a new equation of D_L (Eq.5.8) is done using my analysis of the longitudinal dispersion of rigid vegetation. In above equation, it is assumed that the variations in concentration are sufficiently small over density of rigid vegetation so we can ignore the term contains density of vegetation. Thus, it is also found that the coefficient of dispersion depends on the density of the vegetation but depends strongly on the diameter of the vegetation due to the increase of the surface. The functional relationship between the non-dimensional terms obtained using IBM SPSS Statistics and the predicted equation to determine the dispersion coefficient were found to correlate well with the observed dispersion coefficient.

CHAPTER 6

CONCLUSIONS

The present study deals with the determination of the longitudinal dispersion coefficient in the presence of vegetation in a rectangular channel.

1. The coefficient of dispersion is depended on the diameter of rigid vegetation, when a rigid vegetation of different diameter is kept at a distance from point of injection the dispersion coefficient value increases in magnitude.
2. Coefficient of dispersion depends on the density of the vegetation but depends strongly on the diameter of the vegetation due to the increases of the surface area which affects lateral dispersion In vegetation, the longitudinal dispersion is reduced as the vegetation density increases with a reduction of approximately 30% to 50% when the density is doubled.
3. The percentage difference between the mean velocity and the cloud velocity is greater for the lower Reynolds number. The speed at which the cloud propagates that decrease in the maximum concentration and the resulting concentration profile along the stream which helps in control the pollution in channel.
4. The experiment results obtained in the present study are compared with empirical relationship provided by various researchers. It is found that Fischer routing equation has best fit to our present experiment results. The D_L value which is found experimentally was compared with different empirical equation, and which were nearly matched with the value of D_L calculated from Fischer routing and is followed the same trend as the experimental concentration followed.
5. The functional relationship between the dependent and independent terms is made using SPSS. The correlation coefficient R^2 of the established relationship is 0.991 indicating a good correlation between the predicted and observed dispersion coefficient. The predicted equation which is used to determine the dispersion coefficient associates well with the observed dispersion coefficients values.

REFERENCES

Ahmad, Z., (1997). "Longitudinal Dispersion of Conservative Pollutants in Open Channels". Thesis submitted in fulfilment of the requirement for the degree of Doctor of Philosophy. Thapar Institute of Engg. & Tech. (Deemed University), Patiala, India.

Ahmad, Z., Kothyari, U., and Ranga R., (1999). "Finite Difference Scheme for Longitudinal Dispersion". Journal of Hydraulic Research, 5(2), 1-21.

Asai, K., Fujisaki, K., and Awaya, Y., (2001). Effect of Aspect Ratio on Longitudinal Dispersion Coefficient, in Environmental Hydraulics. (Eds. Lee and Cheung) Vol. 2. Balkema, Rotterdam, the Netherlands, pp. 493-498.

Azamathulla, H.M., Ghani, A., "Genetic programming for predicting longitudinal dispersion coefficients in streams". Water Resour. Manag. 2011, 25, 1537–1544.

Azamathulla, H. M., and Wu, F., (2011). "Support vector machine approach for longitudinal dispersion coefficients in natural streams." Appl. Soft Comp., 11(2), 2902-2905.

Babbar, R., Joshi, H., (2008). "Empirical validation of field estimated dispersion coefficient for a tropical river", Asian Journal of Water, Environment and Pollution, 5(3), 73-78.

Boybeyi, Z.; Ahmad, N.N.; Bacon, D.P.; Dunn, T.J.; Hall, M.S.; Lee, P.C.S.; Sarma, R.A.; Wait, T.R. "Evaluation of the operational multiscale environment model with grid adaptivity against the European tracer experiment". *J. Appl. Meteorol.* **2001**, *40*, 1541–1558.

Bhattacharya, B., and Solomatine, D., (2005). "Neural networks and M5 model trees in modelling water level-discharge relationship." Neurocomp., 63, 381-396.

Brady, J. A., Johnson, P., (1981). "Prediction times of travel, dispersion and peak concentrations of pollution incidents in streams". Journal of Hydrology, 53, 135-150.

Boxall, J. B., Guymer, I. and Marion, A. (2003) "Transverse mixing in sinuous natural open channel flows", J. Hydrology Res., 41(2), 153-165.

Chapra, S.C. Surface Water-Quality Modeling; McGraw-Hill Series in Water Resources and Environmental Engineering: New York, NY, USA, 1997.

Cheng, N.S., and Nguyen, H. T., (2011) “Hydraulic Radius for Evaluating Resistance Induced by Simulated Emergent Vegetation in Open-Channel Flows.” Journal of Hydraulic Engineering. 137 (9): 995 – 1004.

Caplow, T., Schlosser, P. and Ho, D. T. (2004) “Tracer study of mixing and transport in the upper Hudson River with multiple dams”, J. Environ. Eng., 130 (12), 1498-1506

Fischer, H. B., (1967). “The mechanics of dispersion in natural streams”. Journal of Hydraulics division, Proceeding of American Society of Civil Engineering, 93, 187-216.

Fischer, H.B.; List, E.J.; Koh, R.C.Y.; Imberger, J.; Brooks, N.H. Mixing in Inland and Coastal Waters; Academics Press: San Diego, CA, USA, 1979.

Fischer, B.H. “Longitudinal Dispersion in Laboratory and Natural Streams”. California Institute of Technology: Pasadena, CA, USA, 1966.

Guymer, I., Allen, C. M., and Brockie, N. J. W. (2011). “Solute mixing from outfalls during overbank flood conditions”.*Proc., Int. Conf. On Envir. Hydr.*, Hong Kong, 447-452.

Guymer, I., (1998). “Longitudinal dispersion in sinuous channel with changes in shape”. Journal of Hydraulics Engineering, ASCE, 124(1), 33-40

Ishikawa Y, Mizuhara K, Ashida M, (2005): “Drag force on multiple rows of cylinders in an open channel”, Grant-in-aid research project report, Kyushu Univ, Fukuoka, Japan.2015,20:689-693

Kemp JL, Harper DM, Crosa GA, (2004): “The habitat-scale eco-hydraulics of rivers”. Ecol Eng 2000,16(1):17–29.

Kothyari U C, Hashimoto H, Hayashi K, (2009) “Effect of tall vegetation on sediment transport by channel flows”. J Hydraulic Res,47:700–710.

Kubrak, E., Kubrak J, and Rowinski P.M, (2008): “Vertical velocity distributions through and above submerged, flexible vegetation”, Hydrol. Sci.J., 53(4), 905–920.

Lee, M. E., & Seo, I. W. (2007). “Analysis of pollutant transport in the Han River with tidal current using a 2D finite element model”. Journal of Hydro-Environment Research, 1(1), 30-42.

Malki, R. 2009. “The Influence of Saltmarsh Vegetation Canopies on Hydrodynamics in the Iintertidal Zone”. PhD Thesis. Cardiff University.

Murphy, E., Ghisalberti, M. & Nepf, H. (2007) “Model and laboratory study of dispersion in flows with submerged vegetation”. Water Resources Research 43 (5).

Nepf, H., Ghisalberti M, White B, and Murphy E (2007), “Retention time a dispersion associated with submerged aquatic canopies”, Water Resource. Res., 43, W04422.

Nepf, H.M., Vivoni, E.R., (2000). “Flow structure in depth-limited, vegetated flow”. Journal of geophysics research, 105(12), 28547-28557.

Nepf, H. M., Ghisalberti M., (2008). “Flow and transport in channels with submerged vegetation. Acta Geophys, 56 753-777.

Pathak, S.K.; Pande, P.K.; Kumar, S. “Effect of circulation on longitudinal dispersion in open channel”. In Proceedings of the 6th Australasian Hydraulics and Fluid Mechanics Conference, Adelaide, Australia, 5–9 December 1977; pp. 597–600.

Perucca, E., Camporeale, C., & Ridolfi, L. (2009). “Estimation of the dispersion coefficient in rivers with riparian vegetation”. Advances in Water Resources, 32, 78–87.

Seo, I. W., & Song, C. G. (2010). “Specification of wall boundary conditions and transverse velocity profile conditions in finite element modelling”. Journal of Hydrodynamics, Ser. B, 22(5), 633-638.

Sahay, R. R. (2013). “Predicting longitudinal dispersion coefficients in sinuous rivers by genetic algorithm”. Journal of Hydrology and Hydromechanics, 61, 214–221.

Shen, C.; Niu, J.; Anderson, E.J.; Phanikumar, M.S., “Estimating longitudinal dispersion in rivers using acoustic doppler current profilers Adv”. Water Resour. 2010, 33, 615–623.

Singh, S., Ahmad, Z., Kothyari, U. (2010) “Mixing coefficients for longitudinal and vertical mixing in the near field of a surface pollutant discharge”, Journal of Hydraulic Research, 48:1, 91-99.

Singh, S. K., Beck, M. B., (2003). “Dispersion coefficient of streams from tracer experiments data”. Journal of Environment Engineering, ASCE, 126(6), 539-546

Singh, S., Ahmad, Z., Kothyari, U. (2009). “Two-dimensional mixing of pollutants in streams with transverse line slug source”. J. Hydraulic Res. 47(1), 90–99.

Taylor, G. I., (1954). “The dispersion of matter in turbulent flow through a pipe”. Proc. Royal Soc. London Ser A., 219, 189-203.

Tayfur G, Singh V (2005). “Predicting Longitudinal Dispersion Coefficient in Natural Streams by Artificial Neural Network”. Journal of Hydraulic Engineering, 131(11): 991-1000.

Toprak ZF, Cigizoglu HK (2008). “Predicting longitudinal dispersion coefficient in natural streams by artificial intelligence methods”. Hydrological Processes, 22(20): 4106-4129.
Turner Design. (1993) Manual Operating Instructions.

Wahl, T. L., (2000) “Analyzing ADV Data Using ADV”. Joint conference on Water Resource Engineering and Water Resources Planning and Management 75(3) 1-10.

White, B. L. and Nepf, H. M. (2003) “Scalar transport in random cylinder arrays at moderate Reynolds number.” Journal of Fluid Mechanics, (487): 43.

Wenxin H, Chengguang L (2016). “Longitudinal dispersion in open channel flow with suspended canopies”. Water Science & Technology 74(3):211-215

White, B., and H. Nepf (2003), “Scalar transport in random cylinder arrays at moderate Reynolds number”, J. Fluid Mech., 487, 43– 79.

APPENDIX

Diameter of rigid vegetation: 12mm

Spacing: 5cm c/c

Arrangement: staggered

Collection site (from PI): 1m, after and before rigid vegetation and 4m.

Sr. No.	Mean Velocity (cm/sec)	Reynolds Number	Froude Number	Cloud Velocity (m/sec)	tcu (sec)	tcd (sec)	σcu²	σcd²	DL(m^2/s) (Method of Moment)	DL(m^2/s) (Fischer Routing)	RMS (error)
I	II	III	IV	V	VI	VII	VIII	IX	X	XI	XII
WITHOUT ANY RIGID VEGETATION											
1	3.359	4426.322	0.033	0.108	34.344	52.924	46.458	50.448	0.0012	0.0005	22.517
2	7.879	14151.07	0.066	0.051	35.754	75.186	51.642	54.260	0.0001	0.0001	14.485
3	2.411	2459.037	0.027	0.048	33.364	75.374	53.334	56.090	0.0001	0.0001	16.654
WITH RIGID VEGETATION OF ϕ12MM, C-C DISTANCE 5CM IN STAGGERED IN 12 ROWS											
1	3.359	4426.322	0.033	0.028	52.924	123.993	46.458	68.720	0.0001	0.0001	40.427
2	7.879	14151.07	0.066	0.041	75.186	124.218	54.260	64.588	0.0002	0.0001	27.720
3	2.411	2459.037	0.027	0.041	75.374	123.977	56.090	67.705	0.0002	0.0001	13.254
		POST CI AFTER VEGETATION AT DISTANCE 3M AND 4M									
1	3.359	4426.322	0.033	0.046	123.993	167.281	68.720	230.966	0.0040	0.0010	30.759
2	7.879	14151.02	0.066	0.066	124.218	154.464	64.588	149.519	0.0061	0.0020	12.850
3	2.411	2459.037	0.027	0.072	123.977	151.947	51.217	67.705	0.0015	0.0001	11.439

Diameter of rigid vegetation: 12mm

Spacing: 7.5cm c/c

Arrangement: staggered

Collection site (from PI): 1m, after and before rigid vegetation and 4m.

Sr. No.	Mean Velocity (cm/sec)	Reynolds Number	Froude Number	Cloud Velocity (m/sec)	tcu (sec)	tcd (sec)	σcu²	σcd²	DL(m^2/s) (Method of Moment)	DL(m^2/s) (Fischer Routing)	RMS (error)
I	II	III	IV	V	VI	VII	VIII	IX	X	XI	XII
WITHOUT ANY RIGID VEGETATION											
1	2.363780	2998.826	0.023642	0.0658583	29.45175	59.81995	84.94781	195.092	0.007865	0.001	23.03037
2	4.848844	7384.839	0.044263	0.0601785	26.75817	59.99259	45.9835	48.44104	0.00013	0.0005	22.0589
3	7.372085	12406.01	0.064021	0.020490	31.82184	53.83445	55.69212	164.9725	0.09085	0.01	24.3589
WITH RIGID VEGETATION OF ϕ12MM, C-C DISTANCE 5CM IN STAGGERED IN 12 ROWS											
1	2.363780	2998.826	0.024	0.052	48.100	86.487	46.212	109.435	0.002235	0.0005	9.589
2	4.848844	7384.839	0.044	0.053	59.993	97.732	48.441	57.631	0.000341	0.0001	10.257
3	7.372085	12406.01	0.064	0.036	61.834	117.461	38.934	164.972	0.001464	0.0001	7.061
		POST CI AFTER VEGETATION AT DISTANCE 3M AND 4M									
1	2.36	2998.83	0.02	0.03	86.49	146.56	46.21	131.72	0.000788	0.0001	3.25
2	4.85	7384.84	0.04	0.04	97.73	147.93	57.63	152.62	0.001501	0.0005	4.12
3	7.37	12406.01	0.06	0.06	117.46	149.43	38.93	143.66	0.006412	0.004	2.25

Diameter of rigid vegetation: 12mm

Spacing: 10cm c/c

Arrangement: staggered

Collection site (from PI): 1m, after and before rigid vegetation and 4m.

Sr. No.	Mean Velocity (cm/sec)	Reynolds Number	Froude Number	Cloud Velocity (m/sec)	tcu (sec)	tcd (sec)	σcu²	σcd²	DL(m^2/s) (Method of Moment)	DL(m^2/s) (Fischer Routing)	RMS (error)
I	II	III	IV	V	VI	VII	VIII	IX	X	XI	XII
WITHOUT ANY RIGID VEGETATION											
1	0.026	3267.963	0.026	0.075	29.451	56.078	84.887	220.432	0.014	0.005	31.255
2	0.032	5335.040	0.036	0.088	23.167	45.995	59.972	138.264	0.013	0.005	19.855
3	0.015	1581.784	0.018	0.054	84.636	121.492	75.981	129.318	0.002	0.001	36.252
WITH RIGID VEGETATION OF ϕ12MM, C-C DISTANCE 5CM IN STAGGERED IN 12 ROWS											
1	0.026	3267.963	0.026	0.105	56.078	75.079	181.840	220.432	0.001	0.001	17.855
2	0.032	5335.040	0.036	0.048	45.995	88.050	138.264	256.710	0.003	0.001	22.974
3	0.015	1581.784	0.018	0.069	121.492	150.684	129.318	142.670	0.001	0.001	25.855
		POST CI AFTER VEGETATION AT DISTANCE 3M AND 4M									
1	0.026	3267.963	0.026	0.041	75.079	123.726	181.840	300.859	0.002	0.0001	3.092
2	0.032	5335.040	0.036	0.141	88.050	102.222	209.910	256.710	0.003	0.001	9.255
3	0.015	1581.784	0.018	0.252	150.684	158.629	24.820	142.670	0.005	0.001	12.216

Diameter of rigid vegetation: 16mm

Spacing: 5cm c/c

Arrangement: staggered

Collection site (from PI): 1m, after and before rigid vegetation and 4m.

Sr. No.	Mean Velocity (cm/sec)	Reynolds Number	Froude Number	Cloud Velocity (m/sec)	tcu (sec)	tcd (sec)	σcu²	σcd²	DL(m^2/s) (Method of Moment)	DL(m^2/s) (Fischer Routing)	RMS (error)
I	II	III	IV	V	VI	VII	VIII	IX	X	XI	XII
WITHOUT ANY RIGID VEGETATION											
1	7.050	11557.8	0.062	0.056	35.287	70.755	47.795	54.984	0.000322	0.00015	17.510
2	3.027	3904.070	0.030	0.066	31.299	61.602	47.720	76.416	0.000206	0.0001	15.842
3	8.069	15044.32	0.067	0.110	39.901	58.048	71.123	91.084	0.006680	0.003	9.523
WITH RIGID VEGETATION OF ϕ12MM, C-C DISTANCE 5CM IN STAGGERED IN 12 ROWS											
1	7.050	11557.88	0.062	0.055	70.755	107.178	54.984	98.455	0.001799	0.0001	11.521
2	3.027	3904.070	0.030	0.043	61.602	107.794	47.720	141.256	0.001898	0.0001	9.631
3	8.069	15044.32	0.067	0.062	58.048	90.231	39.741	91.084	0.0003	0.00015	18.525
		POST CI AFTER VEGETATION AT DISTANCE 3M AND 4M									
1	7.050	11557.88	0.062	0.072	107.178	134.880	98.455	129.911	0.003	0.001	7.775
2	3.027	3904.070	0.030	0.041	107.794	156.717	141.256	476.019	0.006	0.003	11.696
3	8.069	15044.32	0.067	0.048	90.231	132.285	39.741	117.783	0.002	0.001	4.166

Diameter of rigid vegetation: 16mm

Spacing: 7.5cm c/c

Arrangement: staggered

Collection site (from PI): 1m, after and before rigid vegetation and 4m.

Sr. No.	Mean Velocity (cm/sec)	Reynolds Number	Froude Number	Cloud Velocity (m/sec)	tcu (sec)	tcd (sec)	σcu²	σcd²	DL(m^2/s) (Method of Moment)	DL(m^2/s) (Fischer Routing)	RMS (error)
I	II	III	IV	V	VI	VII	VIII	IX	X	XI	XII
WITHOUT ANY RIGID VEGETATION											
1	6.55531	10265.09	0.0590	0.0477325	36.64593	78.5461	62.27907	74.15883	0.00032	0.00015	24.81172
2	2.294653	2354.588	0.0255	0.0489760	37.69292	78.52924	57.96938	67.14688	0.000269	0.0001	22.89522
3	2.99755	4045.202	0.0291	0.0608978	50.70088	83.54277	60.13997	89.98591	0.000268	0.0001	19.25465
WITH RIGID VEGETATION OF ϕ12MM, C-C DISTANCE 5CM IN STAGGERED IN 12 ROWS											
1	6.55531	10265.09	0.0590	0.0291643	78.5461	147.123	62.27907	101.2575	0.00024	0.0001	9.65821
2	2.294653	2354.588	0.0255	0.0491759	78.52924	119.1995	67.14688	86.7728	0.00058	0.00025	6.134708
3	2.997551	4045.202	0.0291	0.0501471	83.54277	123.4254	60.13997	91.68018	0.000994	0.0005	22.54528
		POST CI AFTER VEGETATION AT DISTANCE 3M AND 4M									
1	6.55531	10265.09	0.0590	0.0925969	147.123	168.722	101.2575	192.4949	0.01810	0.009	9.58421
2	2.294653	2354.588	0.0255	0.097883	103.9715	124.4038	96.85352	149.226	0.01227	0.005	3.25252
3	2.997551	4045.202	0.0291	0.080221	123.3147	148.2457	77.51245	87.12468	0.01240	0.005	2.205225

Diameter of rigid vegetation: 16mm

Spacing: 10cm c/c

Arrangement: staggered

Collection site (from PI): 1m, after and before rigid vegetation and 4m.

Sr. No.	Mean Velocity (cm/sec)	Reynolds Number	Froude Number	Cloud Velocity (m/sec)	tcu (sec)	tcd (sec)	σcu²	σcd²	DL(m^2/s) (Method of Moment)	DL(m^2/s) (Fischer Routing)	RMS (error)
I	II	III	IV	V	VI	VII	VIII	IX	X	XI	XII
WITHOUT ANY RIGID VEGETATION											
1	4.091388	6366.078	0.0370	0.046272	54.90118	98.12323	91.7291	169.8645	0.001935	0.0005	16.78494
2	3.151495	4045.202	0.0313	0.044894	34.80733	79.35579	56.66617	124.9623	0.001544	0.0006	22.2552
3	1.689808	1766.522	0.0186	0.0448737	27.16697	71.73651	52.14323	64.48181	0.000278	0.0001	17.5854
WITH RIGID VEGETATION OF ϕ12MM, C-C DISTANCE 5CM IN STAGGERED IN 12 ROWS											
1	4.09138	6366.078	0.0370	0.0605735	66.45792	99.47565	96.71056	238.9364	0.00790	0.005	7.363772
2	3.151495	4045.202	0.0313	0.0482085	79.35579	120.8422	108.8552	124.9623	0.000451	0.0002	18.2542
3	1.689808	1766.522	0.0186	0.0506241	71.73651	111.2433	64.48181	108.6975	0.001434	0.0005	22.2542
		POST CI AFTER VEGETATION AT DISTANCE 3M AND 4M									
1	4.091388	6366.078	0.0370	0.0536495	99.47565	136.7546	96.71056	166.2535	0.002684	0.001	5.782553
2	3.151495	4045.202	0.0313	0.0493436	88.32791	128.86	82.08475	219.7698	0.004135	0.002	4.25452
3	1.68980	1766.522	0.0186	0.0644551	84.28445	115.3138	79.87788	96.84549	0.001135	0.00065	3.335389

Diameter of rigid vegetation: 20mm

Spacing: 5cm c/c

Arrangement: staggered

Collection site (from PI): 1m, after and before rigid vegetation and 4m.

Sr. No.	Mean Velocity (cm/sec)	Reynolds Number	Froude Number	Cloud Velocity (m/sec)	tcu (sec)	tcd (sec)	σcu²	σcd²	DL(m^2/s) (Method of Moment)	DL(m^2/s) (Fischer Routing)	RMS (error)
I	II	III	IV	V	VI	VII	VIII	IX	X	XI	XII
WITHOUT ANY RIGID VEGETATION											
1	1.93185	3022.721	0.0174	0.0645	36.89	68.54	49.935	75.854	0.001625	0.0005	31.758
2	1.234242	1291.042	0.0136	0.0813	55.821	81.725	185.254	229.35	0.00565	0.0025	9.654
3	4.127063	5980.135	0.0386	0.0568212	34.70959	69.90768	67.847	143.03	0.003448	0.001	4.166
WITH RIGID VEGETATION OF ϕ12MM, C-C DISTANCE 5CM IN STAGGERED IN 12 ROWS											
1	1.931850	3022.721	0.0174	0.0709505	59.18857	87.3772	110.6105	210.6439	0.008932	0.004	18.376
2	1.234242	1291.04	0.0136	0.0956	59.85	80.54	114.251	180.352	0.003251	0.0015	10.263
3	4.127063	5980.135	0.0386	0.0359	112.52	139.85	168.22	196.35	0.00294	0.001	7.256
		POST CI AFTER VEGETATION AT DISTANCE 3M AND 4M									
1	1.931850	3022.721	0.0174	0.0893	51.589	74.5833	154.852	191.254	0.022186	0.001	8.563
2	1.234242	1291.042	0.0136	0.1282522	89.68748	105.2818	130.9959	193.9192	0.033185	0.0015	3.744
3	4.127063	5980.13	0.0386	0.11125	36.584	56.822	112.252	138.922	0.042552	0.0025	9.568

Diameter of rigid vegetation: 20mm

Spacing: 7.5cm c/c

Arrangement: staggered

Collection site (from PI): 1m, after and before rigid vegetation and 4m.

Sr. No.	Mean Velocity (cm/sec)	Reynolds Number	Froude Number	Cloud Velocity (m/sec)	tcu (sec)	tcd (sec)	σcu²	σcd²	DL(m^2/s) (Method of Moment)	DL(m^2/s) (Fischer Routing)	RMS (error)
I	II	III	IV	V	VI	VII	VIII	IX	X	XI	XII
WITHOUT ANY RIGID VEGETATION											
1	6.166031	9992.959	0.0546	0.0585717	53.7031	87.84926	124.5973	175.7213	0.002568	0.001	19.061
2	7.092756	11291.95	0.0633	0.0782	38.3242	52.2545	110.2532	134.586	0.000125	0.05	27.365
3	2.705413	3630.773	0.0263	0.0483	65.2522	89.52323	104.2365	135.236	0.000356	0.00015	32.552
WITH RIGID VEGETATION OF ϕ12MM, C-C DISTANCE 5CM IN STAGGERED IN 12 ROWS											
1	6.166031	9992.959	0.0546	0.035233	64.5866	96.621	76.562	110.5156	0.003532	0.0015	18.622
2	7.09275	11291.9	0.0633	0.0585717	53.7031	124.5973	87.84926	175.7213	0.002568	0.001	20.674
3	2.705413	3630.773	0.0263	0.0325	35.266	61.295	45.695	69.6522	0.004556	0.002	19.685
		POST CI AFTER VEGETATION AT DISTANCE 3M AND 4M									
1	6.166031	9992.959	0.0546	0.0365262	38.6562	64.5842	55.822	81.26258	0.004823	0.002	16.625
2	7.092756	11291.95	0.0633	0.0025685	121.2551	166.6228	117.6299	121.8559	0.001562	0.001	12.68
3	2.705413	3630.773	0.0263	0.0442278	120.0366	165.2569	121.9476	126.1221	0.009028	0.0045	1.683

Diameter of rigid vegetation: 20mm

Spacing: 10cm c/c

Arrangement: staggered

Collection site (from PI): 1m, after and before rigid vegetation and 4m.

Sr. No.	Mean Velocity (cm/sec)	Reynolds Number	Froude Number	Cloud Velocity (m/sec)	tcu (sec)	tcd (sec)	σcu²	σcd²	DL(m^2/s) (Method of Moment)	DL(m^2/s) (Fischer Routing)	RMS (error)
I	II	III	IV	V	VI	VII	VIII	IX	X	XI	XII
WITHOUT ANY RIGID VEGETATION											
1	1.689808	1766.522	0.0186	0.0643824	40.61182	71.67621	114.1088	155.5178	0.00276	0.001	21.436
2	4.137317	6272.872	0.0379	0.095822	32.2589	65.2526	105.2524	143.2555	0.00155	0.0005	32.568
3	1.655342	1766.522	0.0181	0.0663	34.596	61.983	84.5972	98.582	0.00368	0.0015	17.697
WITH RIGID VEGETATION OF ϕ12MM, C-C DISTANCE 5CM IN STAGGERED IN 12 ROWS											
1	1.689808	1766.522	0.0186	0.05983	96.3593	109.683	49.3834	128.653	0.0356	0.015	9.642
2	4.137317	6272.872	0.0379	0.1360182	104.5171	119.221	55.903	139.24	0.0524	0.025	17.615
3	1.65534	1766.522	0.0181	0.05636	36.935	64.65933	109.653	139.6824	0.0425	0.002	35.652
		POST CI AFTER VEGETATION AT DISTANCE 3M AND 4M									
1	1.689808	1766.522	0.0186	0.080267	29.3522	66.369	105.699	176.655	0.02356	0.01	31.789
2	4.137317	6272.872	0.0379	0.05366	50.369	73.689	132.266	191.356	0.0362	0.015	15.986
3	1.655342	1766.522	0.0181	0.0810666	125.6169	150.2879	34.855	149.907	0.0153	0.005	7.925